PIEZOELECTRIC ENERGY HARVESTERS BASED ON POLYCRYSTALLINE PZT AND MONOCRYSTALLINE PMN-PT MATERIALS

PHOSY PANTHONGSY

A THESIS SUBMITTED IN FULFILLMENT
OF THE REQUIREMENT FOR THE DEGREE OF
MASTER OF ENGINEERING IN COMPUTING IN ENGINEERING SYSTEMS
INTERNATIONAL COLLEGE
KING MONGKUT'S INSTITUTE OF TECHNOLOGY LADKRABANG
2015
KMITL-2015-IC-M-11-03

Thesis	Piezoelectric Energy Harvesters Based on Polycrystalline PZT and Monocrystalline PMN-PT Materials
Student	Mr. Phosy Panthongsy
Student ID	57610017
Degree	Master of Engineering
Program	Computing in Engineering Systems
Year	2016
Thesis Advisor	Asst. Prof. Dr. Don Isarakorn

ABSTRACT

The piezoelectric energy harvester for supplying power to low-power electronic devices has been studied and received more attraction over the past decade. In order to simplify installation and obtain the sufficient power for systems, the harvester possessing simple structure with highest output power is highly required. The aim of this thesis is to study on the piezoelectric energy harvesters based on polycrystalline PZT and monocrystalline PMN-PT materials. This research is implemented on comparative study of the unimorph energy harvesters based on polycrystalline PZT and monocrystalline PMN-PT materials, and study of bimorph energy harvesters based on polycrystalline PZT for harvesting energy from machine vibration. By using the finite element analysis (FEA) in ANSYS, the numerical models of resonant type piezoelectric energy harvesters with proof mass are designed and then fabricated. In the comparative study, the performances of unimorph piezoelectric energy harvesters exciting at their resonant frequency of 150 Hz are investigated with the electromagnetic shaker. As the results, the unimorph monocrystalline PMN-PT piezoelectric energy harvester demonstrates a higher generated power at an optimal load resister, which is 500.07 μWg^{-1}, while the piezoelectric polycrystalline PZT unimorph energy harvester demonstrated an output power of 41.20 μWg^{-1}. For the energy harvesting from machine vibration, the resonant frequency of the bimorph piezoelectric energy harvesters are designed to match the frequency of vibration source. The fabricated harvesters are examined with the spinning and rinsing system of the fully automatic dicing saw machine. An optimal energy harvester can generate the output voltage 29.2 V at frequency 50 Hz. Its generated energy is stored in a 2200 μF capacitor. The stored energy reaches to 27.50 mJ in 2507 - 8358 seconds, which is enough for powering wireless sensor node with energy consumption of 13.29 mJ.

ACKNOWLEDGEMENTS

This master thesis would not have been possible without the help, guidance, and support of my supervisor and friends around me, to only some of whom it is possible to give particular mention here. First of all, I would like to sincerely appreciate to my advisor, Asst. Prof. Dr. Don Isarakorn a Head of Multi-Scale Electromechanical System Laboratory, Dr. Pattanaphong Janphuang and Mr. Songmoung Nundrakwang for their professional guidance and support throughout my research at King Mongkut's Institute of Technology Ladkrabang, Thailand.

I am also thankful to AUN/Seed-Net for highly continues support during the time I have been studying for my master degree. I also extend my sincere appreciation to KMITL for giving me the great opportunity to do research in a warm environment.

Furthermore, I would like to thank all of my colleagues all alumnae and present members of the Multi-Scale Electromechanical System Laboratory and acknowledged for their support, helpful discussions and friendship. Finally, I would like to acknowledge all support of my beloved family for their unflagging love, always stand by my side and encourage for everything, have given me their unequivocal support throughout, as always, for which my mere expression of thanks likewise does not suffice. It is their tolerance and love that carry me through the peaks and through in my entire life.

Phosy Panthongsy

TABLE OF CONTENTS

TABLE OF CONTENTS (Cont.)

LIST OF FIGURES

LIST OF FIGURES (Cont.)

LIST OF TABLES

Chapter 1
Introduction

1.1 Motivation

In over the last decade, The wireless sensor technology running on battery is the most commonly utilized for tracing the essential information both in harsh and unreachable environment [1], since the cost is lower than wired solutions due to maintenance, affiliated problem-solving and repair issues. Even though using battery can solve the problem of wiring, it has problem on limited lifetime and energy storage capacity. Therefore, the methods of converting the waste energy available from the ambient environment into usable electrical energy are much challenge and required [2-4]. The available primary energy sources that can be harvested and integrated into the wireless sensor node are solar [5], thermal [6], mechanical vibration [7] and electromagnetic waves [8]. From these energy resources, the mechanical vibrations are very attracted to apply as the potential power source of wireless sensor node on mechanical condition observation because the most of machines always oscillate during operation. The transduction methods for harvesting vibration energy based on electromagnetic [9], electrostatic [10], and piezoelectric conversions [11];

- Electromagnetic energy harvester: It based on electromagnetic induction. An electromotive force is generated from a relative motion between a coil and a magnet.
- Electrostatic energy harvester: A variable capacitor structure is used to generate charges from a relative motion between two plates.
- Piezoelectric energy harvester: The charge is generated from piezoelectric materials under stress/strain.

While each of these generators presents advantages and disadvantages depending on the application (frequencies and amplitudes of vibrations), a quick comparison of approaches is possible by considering the energy density of each type of generators. Such a comparison is reported in Table 1.1 by Roundy *et al.* [12]. From Table 1.1, it demonstrates that piezoelectric converter is capable of producing the highest power output. Therefore, the piezoelectric generator is very interesting to adapt as the autonomous energy source for powering wireless sensor node in order to stabilize the self-powered system operation.

Table 1.1 Comparison of power density

Type	Energy density (mJ/cm^3)
Piezoelectric	35.4
Electromagnetic	24.8
Electrostatic	4.0

1.2 Piezoelectricity

The piezoelectricity was discovered by Pierre and Jacque Curie in 1880. This word means the electricity obtained from pressure; the word "piezo or piezien" comes from the Greek, which signifies "to squeeze or press". The comprehension about piezoelectric effect is a matter concerning to the interaction between mechanical and electrical state in crystalline materials. The electrical charge generation in piezoelectric material resulting from an inputted mechanical force was called the direct piezoelectric effect, and the mechanical deformation resulting from an applied electrical field was called the reverse piezoelectric effect as shown in Figure 1.1 (a) and (b), respectively. This phenomenon is formed in crystal with no center of symmetry. A letter "P" in the image means the direction of polarization. Generally, each contributed molecule on the piezoelectric has an individual polarization with random direction. One end of it is more negative charged and other end is positives charged, which is called a dipole. For the usable piezoelectric, the polarization of all dipoles must lie in one direction. Hence, the polar axis running through the center of both positive and negative charged of molecule is an imaginary line. It is feasible by applying heat to contributed piezoelectric substance under the application of a strong electric field. The heat stimulates the molecules to move more freely and the electric field forces all of the dipoles in the crystal to line up and face in nearly the same direction. This process is called poling, which is illustrated in the Figure 1.2.

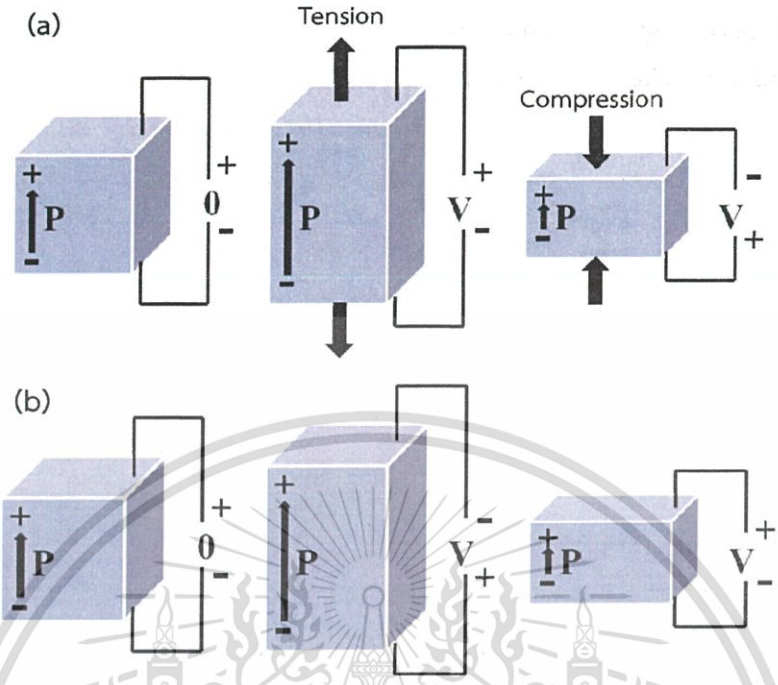

Figure 1.1 (a) Direct piezoelectric effect and (b) reverse piezoelectric effect

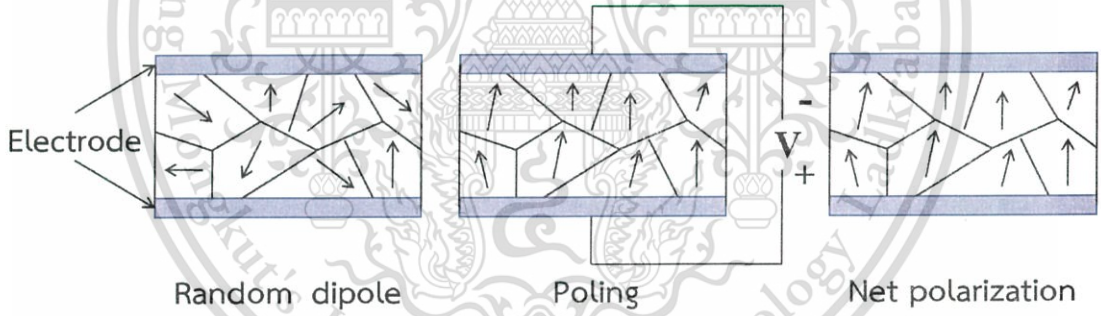

Figure 1.2 Poling process for regulating direction of dipoles

As the above-mentioned phenomenon, the electromechanical interaction of the piezoelectric effect also can be described by following the equations

$$S_j = d_{ij}E_i + s_{ij}^{E}T_j \tag{1.1}$$

$$D_i = d_{ij}T_j + \varepsilon_{ij}^{T}E_i \tag{1.2}$$

where S_j is the mechanical strain resulting from applied electric field (E_i), d_{ij} is the piezoelectric constant interacting to the obtained mechanical strain from inputted applied electric field or stress (T_j), s_{ij}^E is the elastic compliance coefficient at constant electric field, D_i is the electric displacement produced by applied stress, and ε_{ij}^T is the permittivity at constant mechanical strain

From the equation (1.1) and (1.2), (i) subscript illustrates the electrical direction, which is one of the three directions as 1, 2, or 3. (j) subscript demonstrates the mechanical direction, which consists of the six directions. Its value would be the one in the range of 1 to 6 as shown in the Figure.1.3 (a). For example, d_{31} is the piezoelectric constants concerning the mechanical strain produced in the 1- direction by an applied the electric field in the 3-direction. In the other way, when the applied electric field and obtained strain are along the 3-direction, the piezoelectric constant is d_{33} as Figure 1.3 (b), and (c).

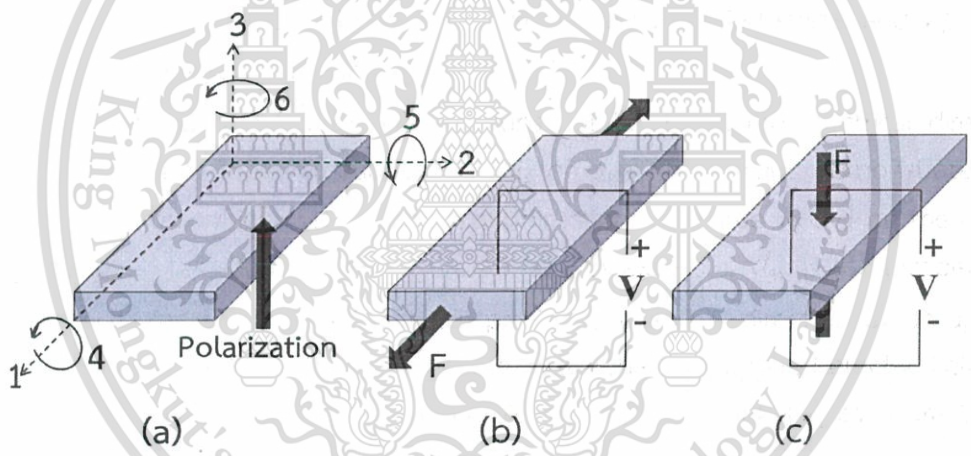

Figure 1.3 (a) Piezoelectric effect direction, (b) 31 (transverse) mode, and (c) 33 (longitudinal) mode

1.3 Research Objectives

The objective of this thesis is to study the piezoelectric energy harvesters based on polycrystalline PZT and monocrystalline PMN-PT materials. The implementation of this research is as follows

- Design and realize the unimorph piezoelectric energy harvesters based on polycrystalline PZT and monocrystalline PMN-PT materials, and then investigate and compare their performance.

- Design and fabricate the bimorph piezoelectric energy harvesters based on polycrystalline PZT for harvesting energy from machine vibration.

1.4 Thesis Overview

By following the research implementation, this thesis is divided into five chapters. Chapter 2 presents the theory of resonant generator leading to understanding of resonant type piezoelectric actions. An equivalent circuit characterizing electrical and mechanical behavior of piezoelectric energy harvester is demonstrated. Moreover, the techniques for harvesters design and estimating the electromechanical performance are also given in this chapter.

The equations providing a guidance of piezoelectric material selection for energy harvesting application, some commonly used piezoelectric materials and the numerical computation of piezoelectric finite elements are proposed in chapter 3.

Chapter 4 gives the design and realization of the polycrystalline PZT and monocrystalline PMN-PT piezoelectric energy harvesters based on unimorph configuration for harvesting energy from the environmental vibration with low frequency excitation. The harvesters are investigated using an electromagnetic shaker exciting as a mechanical vibration input. Energy harvesting performance including mechanical coupling coefficient, quality factor, energy density and generated power are demonstrated and compared in order to obtain the optimal harvester.

The design and fabrication of the polycrystalline PZT piezoelectric energy harvesters based on bimorph configuration are demonstrated in chapter 5. The resonant frequency of harvesters is designed to match the frequency of vibration source in order to obtain the maximum energy generation. The prototype of harvesters are fabricated and tested with the spinning and rinsing system of the fully automatic dicing saw machine (SINGULATION MODEL: DFD 6340). The optimal device is integrated to an energy management circuit for energy storage experiment.

Finally, Chapter 6 summarizes the results of this research and the conclusions from all chapters.

Chapter 2

Resonant Generator and Modeling Method

2.1 Theory of Resonant Generator

The transduction mechanism converting the vibration energy into electrical energy was modeled to base on mass (m) – spring (k) – damper (c) system by Williams and Yates [13] as demonstrated in the Figure 2.1.

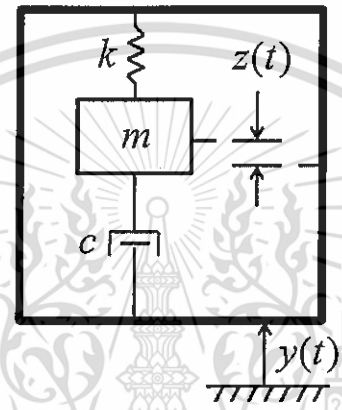

Figure 2.1 Resonant generator model

The ideal of resonant generator is understood as the rigid frame consists of a seismic mass suspended by a spring inside. A mass and spring make the resonant oscillation in transducer. While applying the external force or displacement $y(t)$, a mass moment can cause the deformed frame and converts the mechanical energy into electrical energy. The motive relation of a mass respecting to the frame is represented by $z(t)$. The damping coefficient (c) causing the energy loss consists of the mechanical damping (c_m) and electrical damping (c_e); the mechanical damping according to friction, air resistance etc., and the electrical damping is resulted from the energy transduction. Hence, the damping coefficient (c) is defined as $c = c_m + c_e$. In order to obtain the governing equation of the typical kinetic generator, the mass of vibration source is assumed to be much larger than a mass m to avoid the damper from harvester. By following the description above, the force equivalence is given as

$$m\ddot{z}(t)+(c_m+c_e)\dot{z}(t)+kz(t)=-m\ddot{y}(t) \tag{2.1}$$

The dissipated power in electrical energy conversion is obtained from electrical damping $c_e$with respect to force F_e. The electrical damping force is given by $F_e=c_e\dot{z}$ at velocity v constant [12]. Conversely, at inconstant velocity (v), the generated power is calculated by

$$P=\int_0^v F_e dv \tag{2.2}$$

By replacing $F_e=c_e\dot{z}=c_e v$ in the equation (2.3), it can be written as

$$P=c_e\int_0^v v dv=\frac{1}{2}c_e v^2=\frac{1}{2}c_e\dot{z}^2 \tag{2.3}$$

Assuming that the external vibration exerts a sinusoidal force to the harvester by $y(t)=y_0\cos(\omega t)$, where y_0 is the frame motion amplitude, and ω is the angular vibration frequency. The transfer function of force equivalence in 2.1 can be derived by applying a Laplace transform as

$$Z=\frac{-ms^2}{ms^2+(c_m+c_e)s+k}Y \tag{2.4}$$

where Z is the Laplace transform of mass motion amplitude, Y is the Laplace transform of the frame motion amplitude, and s is the variable parameter of Laplace, which balance to $j\omega$. Hence, the equation (2.3) is rewritten by

$$P=\frac{1}{2}c_e s^2 Z^2 \tag{2.5}$$

According to kinetic theory mass-spring system, if the system has resonant frequency ω_n, the spring constant k is given by $k=m\omega_n^2$. The mechanical and electrical damping are obtained as $c_m=2m\zeta_m\omega_n$ and $c_e=2m\zeta_e\omega_n$ where ζ_m and ζ_e are mechanical and electrical damping ratios, respectively. By substituting these parameters in the equation (2.4) and (2.5), the power can be considered by

$$P = \frac{m\zeta_e \omega_n \omega^2 \left(\frac{\omega}{\omega_n}\right)^3 Y^2}{\left[1-\left(\frac{\omega}{\omega_n}\right)^2\right]^2 + \left[2(\zeta_m+\zeta_e)\left(\frac{\omega}{\omega_n}\right)^2\right]^2} \tag{2.6}$$

while the resonant generator is exciting at its resonant frequency, which matches to the frequency of vibration source. It denotes that the ω_n balances to ω, and an acceleration level can be calculated from $a = \omega^2 Y$. By following this addition and equation (2.6), the power can be obtained as

$$P = \frac{m\zeta_e a^2}{4\omega_n(\zeta_m+\zeta_e)} \tag{2.7}$$

From the equation (2.7), the power will be optimized and maximized when the mechanical damping ratio ζ_m is lowest, and matched to electrical damping ratio ζ_e.

2.2 Resonant Type Piezoelectric Energy Harvester Equivalent Circuit

A general configuration of resonant type piezoelectric energy harvester is composed of a cantilever beam with a proof mass placed at tip as shown in Figure 2.2. The convenient method for simplifying the system equation for modeling generator is to model the electromechanical portion as circuit elements in Figure 2.3. This approach was developed by Roundy *et al.* [14].

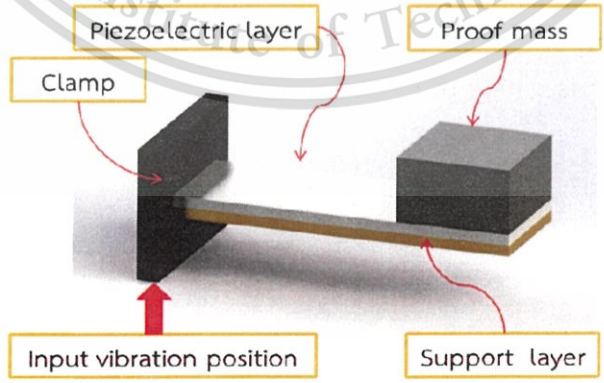

Figure 2.2 Resonant type piezoelectric energy harvester

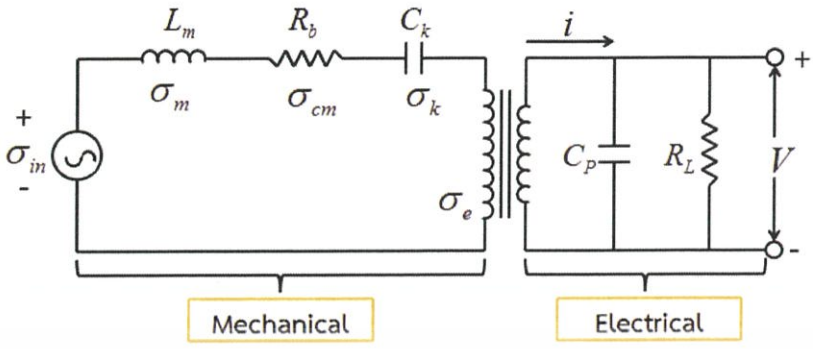

Figure 2.3 Piezoelectric energy harvester equivalent circuit

For the equivalent circuit, the transformer with equivalent turns ratio n is assigned as the electromechanical coupling, an equivalent input stress σ_{in} developed by the input vibration, the equivalent conductor L_m, resistor R_b, and capacitor C_k are represented the mass (m), mechanical damping and mechanical stiffness, respectively. For other side of transformer is electrical equivalent circuit, C_p is the piezoelectric capacitance, and R_L is the load resistance. By considering the equivalent circuit on Kirchoff's Voltage Law, the input stress is derived by

$$\sigma_{in} = \sigma_m + \sigma_{cm} + \sigma_k + \sigma_e \tag{2.8}$$

As following the equation of piezoelectric effect in chapter1,

$$S = dE + s^E \sigma \tag{2.9}$$

$$D = d\sigma + \varepsilon^T E \tag{2.10}$$

where stress σ is represented T in equation (1.1) and (1.2). In the cause of applying stress to electrical field at zero strain or providing the electric displacement to strain at zero electric field, the equation expressing the equivalent circuit performance based on piezoelectric effect is given by

$$\sigma = -\frac{dE}{s^E} = -dY_p E \tag{2.11}$$

$$D = d\sigma = -dY_P S \tag{2.12}$$

where d denotes the piezoelectric strain coefficient, Y_P is the Young's modulus of the piezoelectric material, and then the turns ratio of transformer is defined as $-dY_P$. During the piezoelectric element operating in 31 mode, the generated charge is calculated by multiplying the total dielectric displacement by electrode surface area A as

$$D = -d_{31}\sigma_{AV} = -d_{31}Y_P S_{AV}(Cm^{-2}) \tag{2.13}$$

$$q = A \cdot D = -d_{31}Y_P S_{AV} \cdot A(C) \tag{2.14}$$

on these equations, the σ_{AV} and S_{AV} illustrate the developed average stress and strain in piezoelectric element. Since the capacitance of piezoelectric component is given by $C_p = \frac{\varepsilon A}{t_P}$ where $\varepsilon = \varepsilon_{33}\varepsilon_0$ and t_P represents the thickness of piezoelectric element. So that the generated charge also can be written as

$$q = \frac{-d_{31}Y_P C_P t_P}{\varepsilon} S_{AV} \tag{2.15}$$

During the piezoelectric element deformed and mechanical strain change, the generated current i is derived by

$$i(t) = \frac{dq(t)}{dt} = \frac{-d_{31}Y_P C_P t_P}{\varepsilon} \cdot \frac{dS_{AV}(t)}{dt} \tag{2.16}$$

Supposing that the applied external vibration excites in harmonic, the voltage across the resistive load R_L is calculated by

$$V_{Peak} = \frac{-j\omega d_{31}Y_P t_P}{\varepsilon(j\omega + \frac{1}{R_L C_P})} S_{AV} \Rightarrow |V_{Peak}| = \frac{\omega d_{31}Y_P t_P}{\varepsilon\left(\sqrt{\omega^2 + \frac{1}{(R_L C_P)^2}}\right)} S_{AV} \tag{2.17}$$

and then the generated power on R_L can be easily defined as

$$P_{rms} = \frac{(V_{Peak}/\sqrt{2})^2}{R_L} = \frac{V_{Peak}^2}{2R_L} \tag{2.18}$$

For the energy transfer to load of resonance type piezoelectric, the maximum power can be extracted only when generator is operated with an optimum load. As the force equivalence presented in equation (2.1) and (2.4), the electrical damping affecting to the generator behavior is partly assigned by electrical load, and the balance between electrical and mechanical damping ratio is occurred at maximum power generation, so the optimal load resistance should be matched to the impedance of piezoelectric element at resonant frequency excitation and mechanical damping of generator [15] as

$$R_{opt} = \frac{1}{\omega C_P} \frac{2\zeta}{\sqrt{4\zeta^2 + k_{31}^2}} \tag{2.19}$$

where the k_{31}^2 is the electromechanical coupling efficient, which denotes the energy conversion ability or energy conversion ratio of generator. In the equivalent circuit, the electrical mechanical coupling efficient depends on turn coil ratio of transformer.

2.3 Finite Element Method (FEM) for Modeling Generator

2.3.1 Finite Element Analysis (FEA)

The finite element analysis is a computerized method for modeling the piezoelectric energy harvester and predicting performance. Generally, the available FEA softwares include COMSOL, ABAQUS, and ANSYS. The COMSOL is utilized to verify the analytical model and considering the generated charge from strained piezoelectric element by simulation of the displacement of cantilever, strain distribution, and resonant frequency [16]. In order to estimate the mechanical and electrical performance of the designed piezoelectric energy harvester, Elvin *et al.* [17] used ABAQUS and circuit simulation SPICE for FEA, respectively. In the other way, Zhu *et al.* [18] simplified the FEA of numerical model within single-software by using a coupled piezoelectric-circuit finite element model (CPC-FEM) developed in ANSYS. The CPC-FEM allows for modeling of the piezoelectric generator and analyzing the electromechanical behavior. Moreover, it can be utilized to predict the generated power and optimal load resistance. Because of these consequences, the FEM in ANSYS software were applied in this thesis in order to design and optimize piezoelectric energy harvesters.

2.3.2 Finite Element Analysis Implementation

The geometry model of resonant type piezoelectric energy harvester configured in cantilever with a seismic mass at the tip is shown in Figure 2.4, a cantilever consists of piezoelectric layer and support layer. In ANSYS, the piezoelectric material is represented by SOLID5 element, and the SOLID45 element is used for non-piezoelectric material such steel, tungsten, etc. Using the *Block Lanzcos* mode excitation method for modal analysis implementation, the resonant frequency of geometry model can be defined.

In order to achieve the electromechanical behavior relating to the vibration characteristics, the coupled piezoelectric-circuit finite element model is constructed by connecting the electrodes of piezoelectric elements (SOLID5) to the piezoelectric circuit element (CIRCU94) as illustrated in Figure 2.4, and then analyzed in harmonic excitation. Generally, CIRCU94 is able to model resistors, inductors, capacitors, voltage sources, or current sources. In this model, CIRCU94 is used to model a load resistor estimating the generated power and optimal load resistance [19]. In the simulation, a constant sinusoidal acceleration is applied to the clamped position of cantilever beam while the harvester is generating the output voltage to across a load resistor, the generated power is calculated, and the optimal load resistor is approximated by

$$R_{opt} = \frac{1}{\omega_n C_P} \tag{2.20}$$

where ω_n is represented by the resonant frequency, and C_P denotes the capacitance of the piezoelectric element.

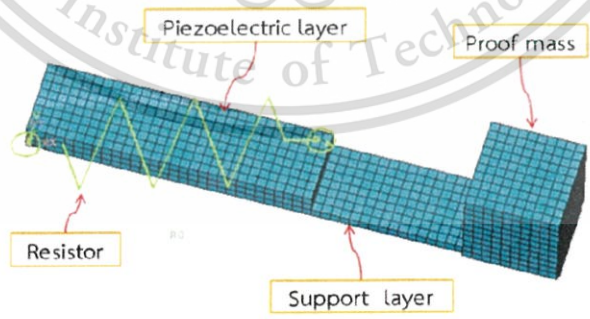

Figure 2.4 Coupled piezoelectric-circuit finite element model of piezoelectric energy harvester

Beside parameters above, the implementation of harmonic analysis requires the constant global damping ratio in numerical calculation for reaching the reliable results. The constant global damping ratio is specified as a decimal number with the DMPRAT command.

2.4 Conclusions

In this chapter, the operation of resonant generator based on mass – spring – damper system for transforming the kinetic energy into electrical energy, and an equivalent circuit of resonant type piezoelectric energy harvester were presented. The relationship between electrical and mechanical behavior through the electronic devices has been demonstrated by an equivalent circuit. In addition, this chapter also mentions the Finite Element Analysis (FEA) and available software for modeling the harvesters such as COMSOL, ABAQUS, and ANSYS.

Chapter 3
Piezoelectric Materials and Numerical Computation

3.1 Selection of Piezoelectric Materials

For the piezoelectric energy harvester, a contributed piezoelectric material has a significantly impact on its achievable performance. The generated voltage, current and power under a cyclic stress (σ_i) are given as [20]

$$V_{3i} = \sigma_i g_{3i} t_i \tag{3.1}$$

$$I_{3i} = \frac{P}{V_{3i}} = \frac{1}{2} d_{3i} \sigma_i A f \tag{3.2}$$

$$P = \frac{1}{2} C_P V_{3i}^2 f = \frac{1}{2} \frac{d_{3i}^2}{\varepsilon_0 \varepsilon^T} \sigma_i^2 t_i A f = \frac{1}{2} (d_{3i} \cdot g_{3i}) \sigma_i^2 t_i A f \tag{3.3}$$

where t_i is the distance between the electrodes, g_{3i} is the piezoelectric voltage constant ($g_{3i} = d_{3i} / \varepsilon^T \varepsilon_0$), d_{3i} is the piezoelectric strain constant, ε^T is the relative dielectric constant at constant stress, ε_0 is the permittivity of free space ($\varepsilon_0 = 8.85 \times 10^{-12}\ F/m$), and C_P is the capacitance of the piezoelectric material, A is the area of the electrodes.

From equation (3.1) and (3.2), the generated voltage and current under a cyclic excitation depend on the g_{3i} constant and d_{3i} constant, respectively. In addition, in an equation (3.3), the generated power depended on the product of ($d_{3i} \cdot g_{3i}$) of the piezoelectric material. The parameters of g_{3i}, d_{3i} and ($d_{3i} \cdot g_{3i}$) can provide a guidance of material selection for energy harvesting application. To choose the piezoelectric materials in this thesis, some commonly used piezoelectric materials are considered and listed in Table 3.1. As can be seen, the PMN-PT and PZT materials are very interested than other piezoelectric materials due to the overall capability of voltage, current and power generation. Therefore, they are selected to study on energy harvesting performance.

Table 3.1 Properties of piezoelectric materials

Piezoelectric materials	ε^T	d_{31} (10^{-12}m/V)	g_{31} (10^{-3}Vm/N)	$d_{31} \cdot g_{31}$ (10^{-12}m^2/N)
AlN [21]	10.5	-1.73	-18.62	0.03
ZnO [22]	11	-5	-51.36	0.25
BaTiO3 [23]	1700	-78	-5.18	0.40
PZT [27]	1000	−97	-10.96	1.06
PMN-PT [27]	8250	−1338	-18.33	24.51

3.2 Piezoelectric Finite Elements

In linear piezoelectric material, the equations of elasticity are coupled to the charge equation of electrostatics as [24]

$$\{T\} = [c^E]\{S\} - \left[e^T\right]\{E\} \tag{3.4}$$

$$\{D\} = [e]\{S\} - \left[\varepsilon^S\right]\{E\} \tag{3.5}$$

where

$\{T\}$ = Vector of mechanical stress ($\{T_{11}T_{22}T_{33}T_{23}T_{13}T_{12}\}$)

$\{S\}$ = Vector of mechanical strains ($\{S_{11}S_{22}S_{33}S_{23}S_{13}2S_{12}\}$)

$\{E\}$ = Vector of electric field ($\{E_1E_2E_3\}$)

$\{D\}$ = Vector of dielectric displacement ($\{D_1D_2D_3\}$)

$[c^E]$ = Mechanical stiffness matrix for a constant electric field E

$\left[\varepsilon^S\right]$ = Dielectric constant matrix for constant mechanical strain S

$[e]$ = Piezoelectric coupling coefficients matrix

$\left[e^T\right]$ = Piezoelectric matrix relating stress/electric field (transposed)

By following the Hamilton principle, the dynamic equations of a piezoelectric continuum can be derived, in which the Lagrangian and the virtual work are properly adapted to include the electrical contribution as well as the mechanical ones. The potential energy density of a piezoelectric material consists of a contribution from the

strain energy and the electrostatic energy [25]. The electric field E relating to electrical potential ϕ is given by

$$E = -grad\phi \tag{3.6}$$

and the mechanical strain S to the mechanical displacement u in the Cartesian coordinates by

$$S = \begin{bmatrix} \partial/\partial_x & 0 & 0 & \partial/\partial_y & 0 & \partial/\partial_z \\ 0 & \partial/\partial_y & 0 & \partial/\partial_x & \partial/\partial_z & 0 \\ 0 & 0 & \partial/\partial_z & 0 & \partial/\partial_y & \partial/\partial_x \end{bmatrix}^T \{u\} = [B]\{u\} \tag{3.7}$$

The elastic behavior of piezoelectric media is governed by Newton's law

$$div\{T\} = \rho \frac{\partial^2 \{u\}}{\partial t^2} \tag{3.8}$$

where ρ presents the density of the piezoelectric medium, whereas the electrical behavior is explained by Maxwell's equation, taking into account the fact that the piezoelectric media are insulating (no free volume charge)

$$div\{D\} = 0 \tag{3.9}$$

Equations (3.4) to (3.9) constitute a complete set of differential equations, which can be solved with the appropriate mechanical (displacement and forces) and electrical (potential and charge) boundary conditions. An equivalent description of above boundary-wave problem is Hamilton's variational principle as extended to piezoelectric media

$$\delta \int_{t_1}^{t_2} (L + W) dt = 0 \tag{3.10}$$

where the operator δ presents the first-order variation, t_1 and t_2 define the time interval (all variations must vanish at $t = t_1$ and $t = t_2$) and the Lagrangian term L is

determined by the energies available in the piezoelectric medium and W is the virtual work of the external mechanical and electrical forces [25-27].

In the Finite Element method the object to be computed is subdivided into small, discrete elements, the so-called Finite Elements. The mechanical displacement u and the forces f as well as the electrical potential ϕ and the charge q are determined at the nodes of these elements. The values of these mechanical and electrical quantities at an arbitrary position on the element are given by a linear combination of the polynomial interpolation function $N(x,y,z)$ and the nodal point values of these quantities as a coefficient. For an element with n nodes (nodal coordinates: (x_i,y_i,z_i), (i=1,2,...,n) the continuous displacement function $u(x,y,z)$ (vector of order three), for example, can be evaluated from its discrete nodal point vectors as follows (the quantities with "0" are the nodal point values of one element):

$$\{u(x,y,z)\}=[N_u(x,y,z)]\{{}^0u(x_i,y_i,z_i)\} \tag{3.11}$$

$$\phi=[N_\phi(x,y,z)]\{{}^0u(x_i,y_i,z_i)\} \tag{3.12}$$

Where $\{{}^0u\}$ is the vector of the nodal point displacement, and $[N_u]$ is the interpolation function for the displacement. Therefore, the strain field $\{S\}$ and the electric field $\{E\}$ are related to the nodal displacement and potential by the shape function derivatives $[B_u]$ and $[B_\phi]$ defined by, [28]

$$\{S\}=[B_u]\{{}^0u_i\} \tag{3.13}$$

$$\{E\}=-[B_\phi]\{{}^0u_i\} \tag{3.14}$$

The substitution of the polynomial interpolation function into (3.11) yields a set of linear differential equations that describe a single piezoelectric finite element.

$$\{M\}\{{}^0\ddot{u}_i\}+[K_{uu}]\{{}^0u_i\}+[K_{u\phi}]\{{}^0\phi_i\}=\{{}^0f_i\} \tag{3.15}$$

$$[K_{\phi u}]\{{}^0u_i\}+[K_{\phi\phi}]\{{}^0\phi_i\}=\{{}^0q_i\} \tag{3.16}$$

Each element k of the mesh is connected to its neighboring elements at the global nodes and the displacement is continuous from one element to the next. The element degrees of freedom (DOF) ($\{{}^0u_i\}$ and $\{{}^0\phi_i\}$) are related to the global DOF ($\{u\}$ and $\{\Phi\}$) by the mean of the localization matrices $[{}^0L_u]$ and $[{}^0L_\phi]$

Hamilton's principle (3.10) must be verified for the whole structure, which results in (by summation of the contribution from each finite element) [24-27, 29].

$$\{M\}\{\ddot{U}\}+[K_{UU}]\{U\}+[K_{U\Phi}]\{{}^0\Phi\}=\{F\} \tag{3.17}$$

$$[K_{\phi U}]\{U\}+[K_{\Phi\Phi}]\{\Phi\}=\{Q\} \tag{3.18}$$

where the assembled matrices are given by

$[M]=\sum_i[L_{ui}]^T[M^{(i)}][L_{ui}]$ is kinematically consistent mass matrix

$[K_{uu}]=\sum_i[L_{ui}]^T[K_{uu}{}^{(i)}][L_{ui}]$ is stiffness matrix

$[K_{u\Phi}]=\sum_i[L_{ui}]^T[K_{u\phi}{}^{(i)}][L_{\phi i}]$ is piezoelectric "stiffness" matrix

$[K_{\Phi U}]=\sum_i[L_{\phi i}]^T[K_{\phi u}{}^{(i)}][L_{ui}]$ is transponse piezoelectric "stiffness" matrix

$[K_{\Phi U}]=\sum_i[L_{\phi i}]^T[K_{\phi u}{}^{(i)}][L_{ui}]$ is dielectric "stiffness" matrix

$\{F\}=\sum_i[L_{ui}]^T[f_i]$ is external forces applied to the structure

$\{Q\}=\sum_i[L_{\phi i}]^T[q_i]$ is electrical charges brought to the electrodes

Equations (3.17) and (3.18) couple the mechanical variables $\{U\}$ and the electrical potentials $\{\Phi\}$. Based on this formulation, a piezoelectric Finite Element of the type multilayered Mindlin shell and volume has been derived [24-25]. For shell elements, it is assumed that the electric field and the displacement are uniform across

the thickness and aligned on the normal to the mid-plane. The electrical degrees of freedom are the voltages ϕ_k across the piezoelectric layers; it is assumed that the voltage is constant over each element (this implies that the finite element mesh follows the shape of the electrodes). One electrical degree of freedom of the type voltage per piezoelectric layer is defined. The assembly takes into account the equipotentiality condition of the electrodes; this reduces the number of electric variables to the number of electrodes. For volume elements, one additional degree of freedom of the type electric potential is introduced in each node of the piezoelectric volume element.

3.3 Conclusions

In this chapter, the commonly used piezoelectric materials and the equations guiding to select the piezoelectric materials for energy harvesting application are demonstrated. The parameters impacting to the generated voltage, current and power of piezoelectric material are considered. On the other hand, the numerical computation of piezoelectric finite elements is also reported.

Chapter 4

Comparative Study of Piezoelectric Energy Harvesters Based on Polycrystalline PZT and Monocrystalline PMN-PT Materials

4.1 Conceptual Model

In order to simplify generator configuration, the conceptual model consisting of a piezoelectric unimorph cantilever and clamped beam is designed as shown in Figure 4.1. To prevent the crack of piezoelectric, a base of cantilever is attached to acrylic using mixed resin. Since the high temperature from soldering makes the piezoelectric property change, thus a PCB clip is directly pinned to piezoelectric surface avoiding these issues. A piezoelectric unimorph cantilever composes of a piezoelectric layer bonded to an elastic layer; made of stainless steel plate. An elastic support layer acting as a spring stimulates the neutral plane away from the center of piezoelectric layer thickness. It causes the net charges to be collected. A tungsten proof mass is placed at the tip of elastic beam for tuning the natural frequency of harvester.

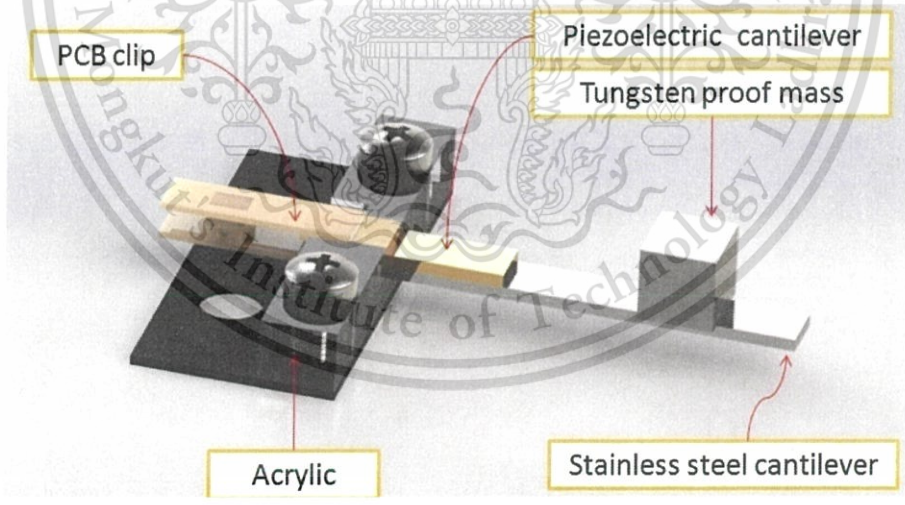

Figure 4.1 A conceptual model of unimorph piezoelectric energy harvesters

4.2 Consideration of Models

4.2.1 Resonant Frequency

For the harvesters design, resonant frequency of piezoelectric harvesters is one of the most important parameter. Amount of generated power would be maximized when natural frequency of energy harvesting device matches the frequency of vibration source. Since many vibration sources from ambient environment excite between 60 Hz and 200 Hz as shown in a Table 4.1. Therefore, the harvesters are designed to have resonant frequency of 150 Hz that lower than 200 Hz; this frequency doesn't derive from any ambient vibration, which is assumed for this research only. If these harvesters are needed to use for harvesting energy from another vibration source, their resonant frequency must be tuned to match the frequency of vibration source.

Table 4.1 Acceleration magnitude and peak frequency of various sources [30]

Vibration source	Acceleration (m/s^2)	Peak frequency (Hz)
Car engine compartment	12	200
Base of 3-axis machine tool	10	70
Blender casing	6.4	121
Clothes dryer	3.5	121
Person nervously tapping their heel	3	1
Car instrument panel	3	13
Door frame just after door closes	3	125
Small microwave oven	2.5	121
HVAC vents in office building	0.2–1.5	60
Windows next to a busy road	0.7	100
CD on notebook computer	0.6	75
Second story floor of busy office	0.2	100

4.2.2 Harvester Components

The piezoelectric elements contributed on this model have a fixed dimension (1 x 4 x 15 mm^3); this scale was fixed by manufacturer, thus the size of support layer and mass effecting to resonant frequency of harvesters should be considered in order to achieve the appropriate models for study of energy harvesting performance. The suitable size of support layer can be obtained by implementing the modal analysis. In simulation,

the piezoelectric and physical properties in Table 4.2 are contributed to geometry model in Figure 3.2 for reaching the reliable results.

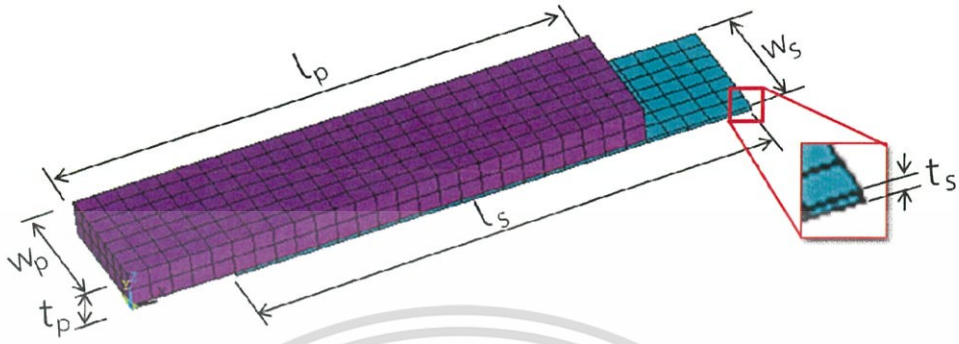

Figure 4.2 Geometry of harvesters without a proof mass for analyzing the reaction of support layer scale

Table 4.2 Piezoelectric and physical properties for numerical model simulation [31]

Physical and Piezoelectric Properties	Piezoelectric Polycrystalline PZT	Piezoelectric Monocrystalline PMN-PT	Stainless Steel Cantilever (SUS304)	Tungsten
Density (kg m^{-3})	7600	8100	8000	19600
Young's Modulus (GPa)	—	—	190	400
Poisson's Ratio	—	—	0.28	0.28
Piezoelectric Charge Constant [10^{-12} C/N]	d_{31} = −97 d_{33} = 225 d_{15} = 330	d_{31} = −1338 d_{33} = 2820 d_{15} = 146	—	—
Relative Dielectric Constant [ε_0]	ε_{11} = 1290 ε_{33} = 1000	ε_{11} = 1600 ε_{33} = 8250	—	—

Table 4.2 (Cont.)

Physical and Piezoelectric Properties	Piezoelectric Polycrystalline PZT	Piezoelectric Monocrystalline PMN-PT	Stainless Steel Cantilever (SUS304)	Tungsten
Elastic Compliance Constant [10^{-12} m^2/N]	S_{11}^E = 11.5 S_{12}^E = −3.7 S_{13}^E = −4.8 S_{33}^E = 13.5 S_{44}^E = 31.9 S_{66}^E = 35.0	S_{11}^E = 70.2 S_{12}^E = −13.1 S_{13}^E = −56.0 S_{33}^E = 119.4 S_{44}^E = 14.5 S_{66}^E = 15.2	—	—

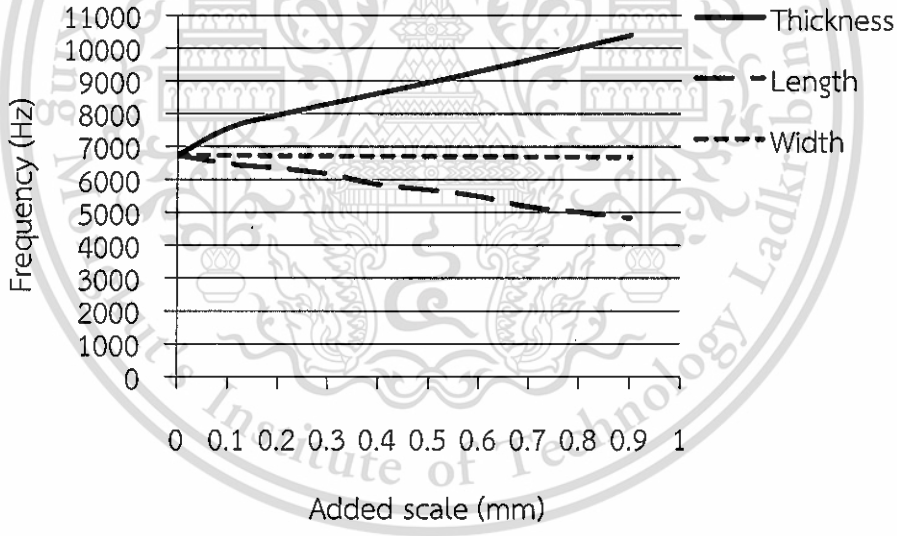

Figure 4.3 Resonant frequency of unimorph polycrystalline PZT piezoelectric energy harvester while increasing the scale of support layer.

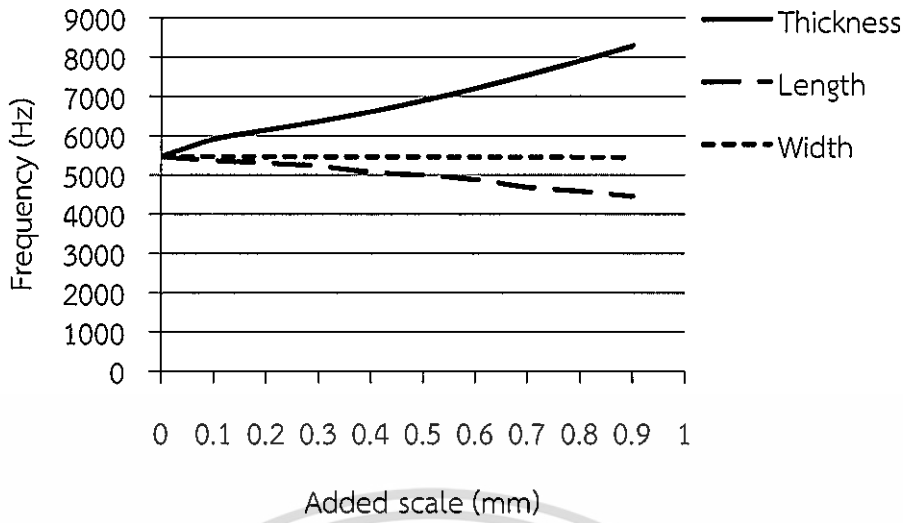

Figure 4.4 Resonant frequency of the monocrystalline PMN-PT piezoelectric energy harvester while increasing scale of support layer.

As shown in the simulation results in Figure 4.3 and 4.4, the thickness of support layer is great impact on frequency of piezoelectric energy harvester, which is directly proportional to the frequency. While increasing thickness from 0.1–0.9 mm and the width and length are kept constant, the resonant frequency of polycrystalline PZT and monocrystalline PMN-PT piezoelectric unimorph cantilever significantly increased. Conversely, the frequency is dropped when a length was increased by 0.1 to 0.9 mm. It is reversely proportional to length as placing a proof mass around the tip end of support layer. Out of this, the frequency almost never changes by increasing width.

Since the increase of length can be replaced by placing a proof mass at the tip end of support layer, and a width have no effect in frequency of harvester. Hence, a width is defined in 4mm for accommodating a piezoelectric element, and a length is 40 mm for simplifying frequency adjustment while moving a proof mass as shown in Figure 4.5. To consider the suitable harvesters, three dimensions of support layer as given in Table 4.3 are diagnosed. They are bonded to piezoelectric elements and then placed a proof mass for tuning the 150 Hz resonant frequency. The composite unimorph piezoelectric energy harvesters can be obtained as show in Table 4.4, and their resonant frequencies are show in Figure 4.6. As the simulation results, the piezoelectric unimorph harvester consisting of support layer volume (0.1 x 4 x 40) mm^3 is not a suitable model because a support layer is more pliable and unable to bend a piezoelectric element. A piezoelectric unimorph cantilever without a proof mass can excites only 126 Hz. A model

consisting of a support layer volume (0.9 x 4 x 40) mm^3 cannot bend by applying accelerations of the harvestable vibration source because a thickness of support layer is large and more stiffness. Furthermore, the piezoelectric element will be broken if apply the heavy force at the tip of support layer. This issue can be observed from a large proof mass that use for decreasing the frequency of harvesters. Among of simulated harvester models, the piezoelectric harvester composing of a support layer volume (0.5 x 4 x 40) mm^3 is more suitable than others. To find out the vibration mode of harvesters bellowing 200 Hz for study of energy harvesting performance, their first four vibration modes are examined as shown in Figure 4.7.

Table 4.3 Composite unimorph piezoelectric energy harvesters.

Numerical Models	Piezoelectric Layer (Polycrystalline and Monocrystalline) Volume (t_p x w_p x l_p) mm^3	Stainless steel Layer Volume (t_s x w_s x l_s) mm^3	Mass (Tungsten) Volume (t_m x w_m x l_m) mm^3
1	1x 4 x 15	0.1 x 4 x 40	0
2	1x 4 x 15	0.5 x 4 x 40	6 x 6 x 6
3	1x 4 x 15	0.9 x 4 x 40	8 x 8 x 15

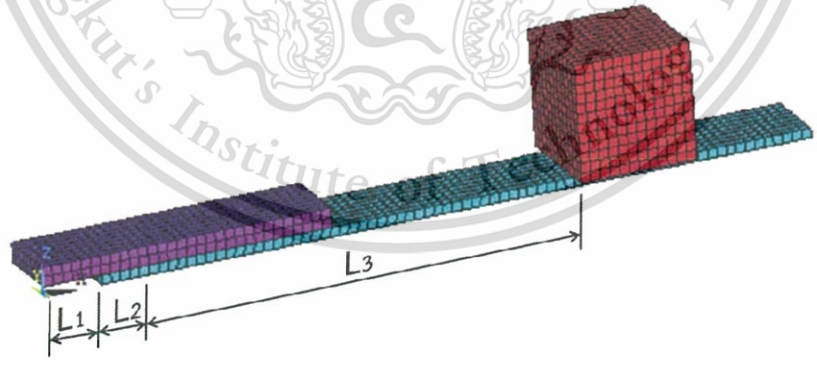

Figure 4.5 Configuration of piezoelectric unimorph energy harvester.

Table 4.4 Parameters setup of composite unimorph piezoelectric energy harvesters.

Numerical Model of Piezoelectric Unimorph Energy Harvesters	Stainless steel layer volume ($t_P \times w_P \times l_P$) mm^3	Clipped Length of PCB, L_1 (mm)	Clamped Length of Base, L_2 (mm)	Placed Length of Proof mass, L_3 (mm)
Polycrystalline PZT	0.1 x 4 x 40	3	3	0
	0.5 x 4 x 40	3	3	25.41
	0.9 x 4 x 40	3	3	21.16
Monocrystalline PMN-PT	0.1 x 4 x 40	3	3	0
	0.5 x 4 x 40	3	3	24.65
	0.9 x 4 x 40	3	3	19.78

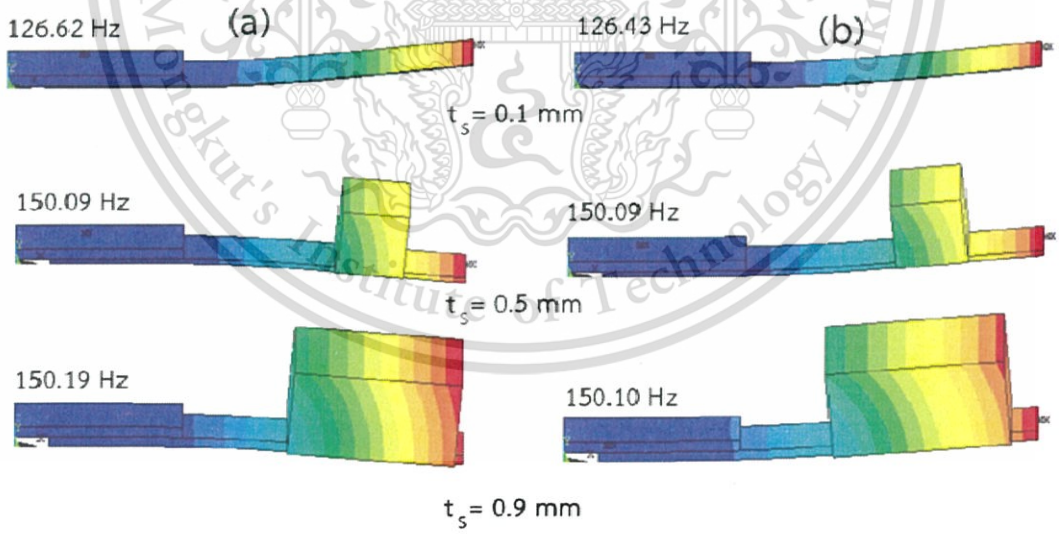

Figure 4.6 Simulated resonant frequency of unimorph (a) polycrystalline PZT and (b) monocrystalline PMN-PT piezoelectric energy harvesters

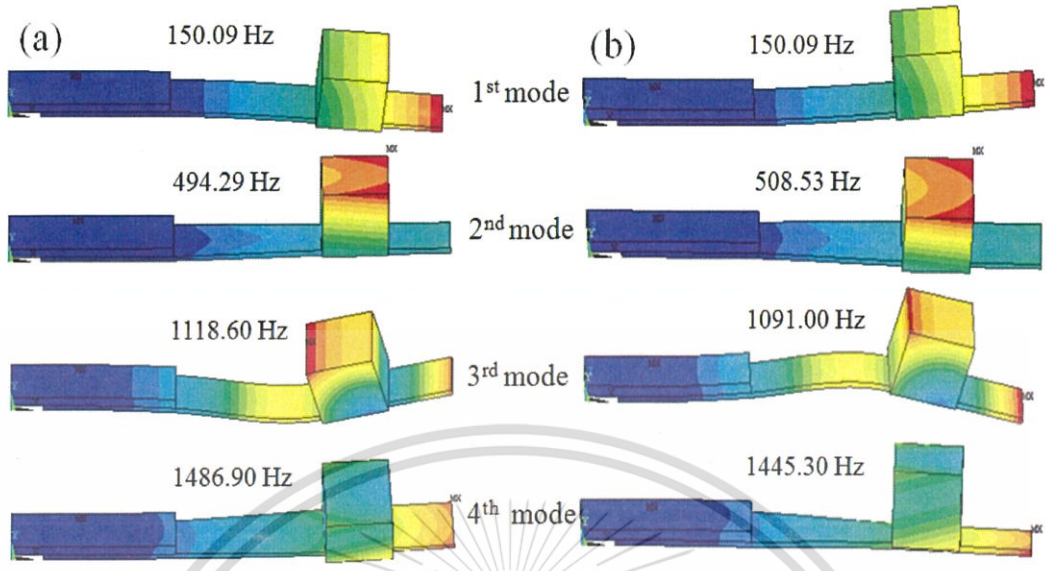

Figure 4.7 Vibration mode shapes of the unimorph (a) polycrystalline PZT and (b) monocrystalline PMN-PT piezoelectric energy harvester.

4.3 Prototypes of Piezoelectric Energy Harvesters

Following the modal analysis of numerical models, both polycrystalline PZT and monocrystalline PMN-PT piezoelectric energy harvesters consisting of support layer volume (0.5 x 4 x 40) mm^3 are fabricated as shown in Figure 4.8. The usable prototypes are confirmed using the electromechanical impedance technique for measuring their resonant frequency. In measurement, an impedance analyzer (Type Bode100) sweeps the frequencies from 100 – 200 Hz with 1 V_{rms} to harvesters.

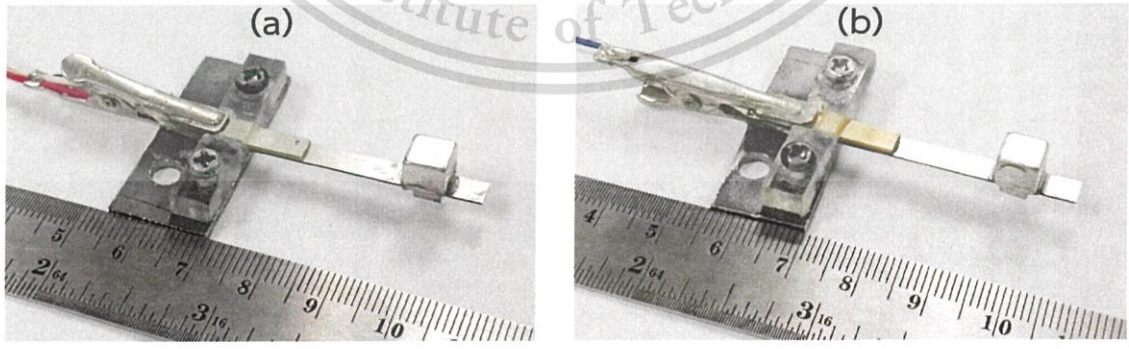

Figure 4.8 (a) polycrystalline and (b) monocrystalline piezoelectric harvesters

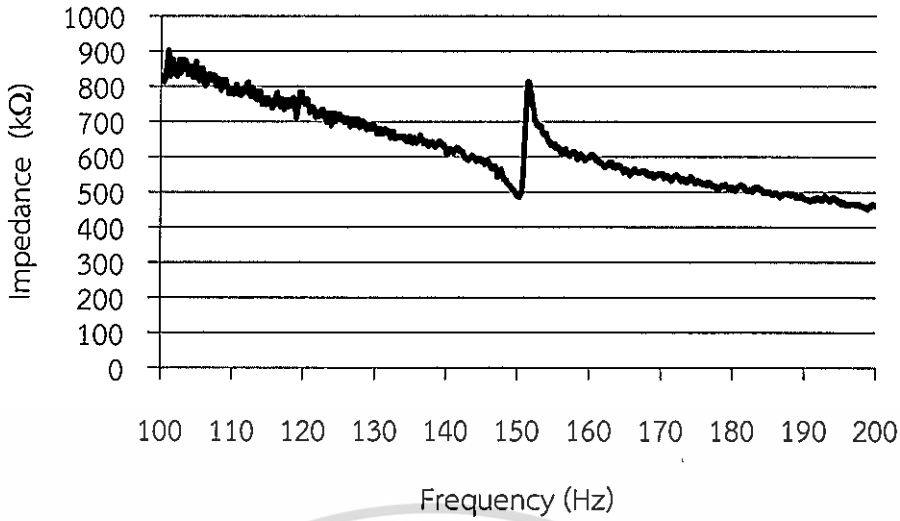

Figure 4.9 Impedance measurement result of unimorph polycrystalline PZT piezoelectric energy harvester.

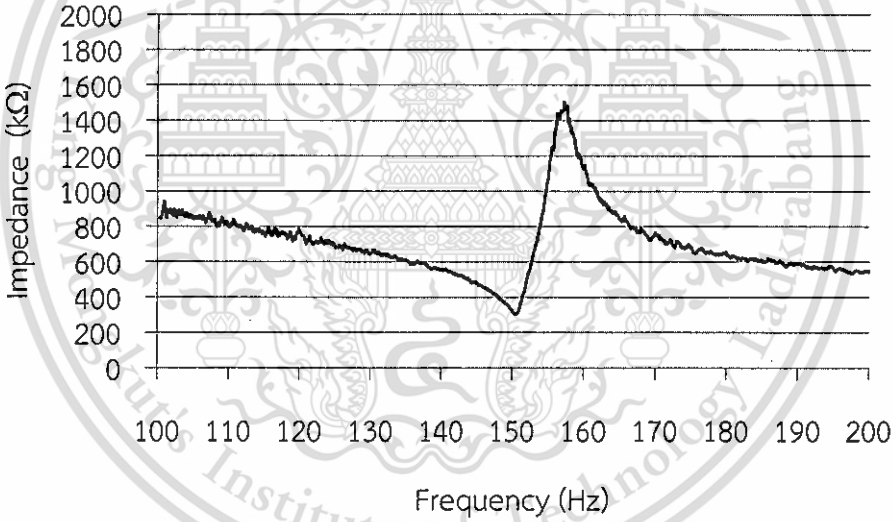

Figure 4.10 Impedance measurement result of unimorph monocrystalline PMN-PT piezoelectric energy harvester.

In Figure 4.9 and 4.10, the measurement results were resonant frequency and anti-resonance frequency. The resonance frequencies of unimorph polycrystalline PZT and monocrystalline PMN-PT piezoelectric energy harvesters resonate at the lowest impedance where 150.33 Hz and 150.48 Hz, and anti-resonant frequencies vibrate at the

maximum impedance as 151.51 Hz and 157.20 Hz, respectively. In this case, the electromechanical coupling coefficient describing the conversion efficiency between mechanical and electrical energy in piezoelectric material can be found by utilizing an equation

$$k_{eff}^2 = 1 - \left(\frac{f_r}{f_a}\right)^2 \tag{4.1}$$

where, k_{eff} is the mechanical coupling coefficient, f_r is the resonant frequency, and f_a is anti-resonant frequency of harvester.

4.4 Energy Harvesting Experimental Setup

To investigate the energy harvesting performance of unimorph piezoelectric energy harvesters, their prototypes are mounted to an electromagnetic shaker (Bruel & Kjaer type 4810). Vary acceleration levels from 0.1–0.5 g and excitation frequencies during 120–180 Hz applying as the mechanical vibration input to harvesters are driven by a power amplifier (Type 2706) and a function generator (Agilent type 33120A). An accelerometer is attached to vibration source for monitoring the magnitude of accelerations, and frequencies as show in Figure 4.11.

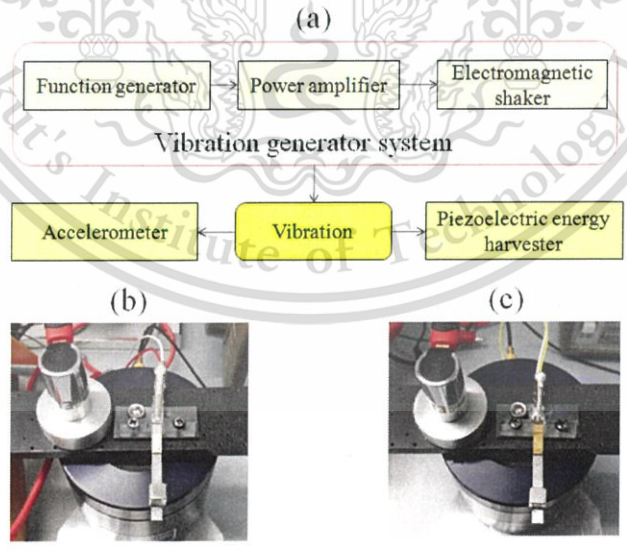

Figure 4.11 (a) A flow chart of energy harvesting experimental setup, and the prototype of unimorph (b) polycrystalline PZT and (c) monocrystalline PMN-PT piezoelectric energy harvesters.

4.5 Experimental Results and Discussion

As the energy harvesting experiment results of the prototypes of unimorph polycrystalline PZT and monocrystalline PMN-PT piezoelectric energy harvesters are illustrated in the Figure 4.12 and 4.13. The frequency of harvesters is decreased by increasing the acceleration magnitude of vibration source. It demonstrates that the young's modulus of harvesters was reduced. The cause of this decrease was depended on the limitation of piezoelectric compliance under heavy stress [32]. While an electromagnetic shaker vibrate at 0.1 g acceleration, unimorph polycrystalline PZT and monocrystalline PMN-PT piezoelectric energy harvesters generate the maximum AC voltage 4.09 V and 18.11 V at 150 Hz. By shaking 0.5 g acceleration, the generated maximum AC voltages are 15.78 V and 84.65 V at 144.50 Hz and 148.00 Hz, respectively.

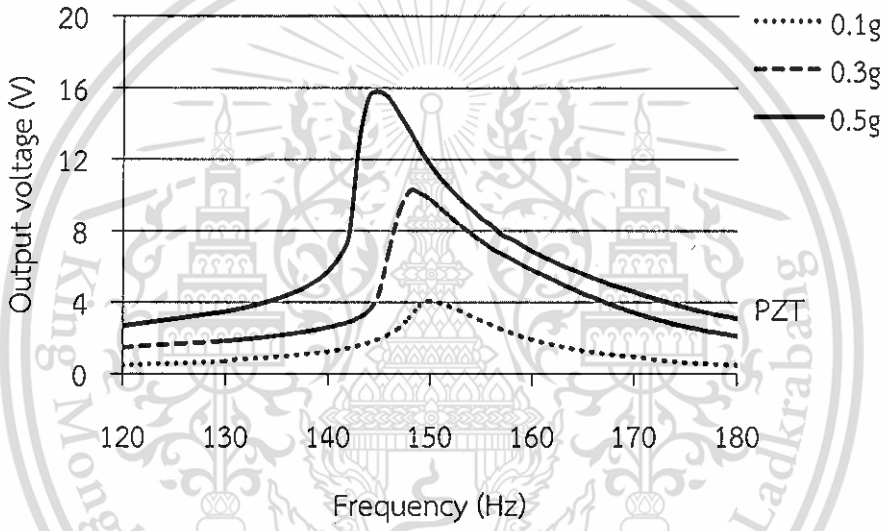

Figure 4.12 Generated output voltage of unimorph polycrystalline PZT piezoelectric energy harvester.

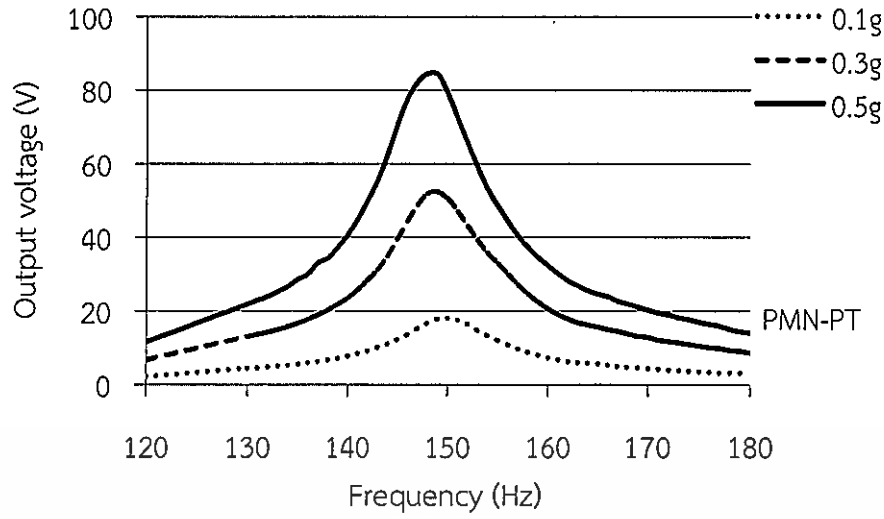

Figure 4.13 Generated output voltage of unimorph monocrystalline PMN-PT piezoelectric energy harvester.

One of the most important parameters for considering the energy transduction capacity of the resonant type piezoelectric energy harvesters is quality factor (Q). The Q factor is estimated by

$$Q = \frac{f_r}{f_2 - f_1} \tag{4.2}$$

where, f_r is the resonant frequency of harvester, and $f_2 - f_1$ is the range of frequency values (bandwidth) where the 0.707 times of the generated voltage amplitude at resonant frequency.

From an equation (4.2), a high Q factor obtaining from a narrow bandwidth demonstrates that the harvester is very sensitive to the vibration change and can harvest energy in a narrow frequency range around the resonant frequency. A low Q factor presents the harvestable energy in the large frequency range about the resonant frequency range due to a large bandwidth frequency. The unimorph polycrystalline PZT and monocrystalline PMN-PT piezoelectric energy harvesters have the average quality factor as 17.59 and 15.70, respectively.

Since the characteristics of piezoelectric energy harvesters are fundamentally capacitor, their capacitances were found for examining the generated energy by using an equation

$$C_p = \varepsilon_r \varepsilon_0 \frac{A}{t} \tag{4.3}$$

where, C_p is the capacitance of harvesters, ε_r is the relative dielectric constant, ε_0 is the permittivity of free space (ε_0 = 8.85 x 10^{-12} F/m), A is a piezoelectric surface area (electrode surface area), and t is a thickness of piezoelectric (thickness separating the electrodes).

Instead of random optimal load resistance range in experiment, the numerical models of harvesters were implemented in harmonic analysis for predicting the optimal load resistor. As a mention in chapter 2, applying the constant global damping ratio (ζ) in numerical calculation leads to achieve the reliable results. Hence, it was found by following an equation

$$\zeta = \frac{f_2 - f_1}{2 f_r} \tag{4.4}$$

In Figure 4.14 and 4.15, By employing the resistance range as simulation for experiment, the maximum power of the unimorph polycrystalline and mono-crystalline piezoelectric energy harvesters can be transferred to a load resistor 0.49 and 1.25 MΩ, where 20.72 and 250.04 μW, respectively. The power transferring to load resistors are extracted from the voltage and current across load resistors as shown in Figure 4.16 and 4.17 by utilizing an equation

$$P_L = V_L I_L \tag{4.5}$$

where P_L presents the generated power on load resistor, V_L is the voltage across load resistor, and I_L is the current across load resistor.

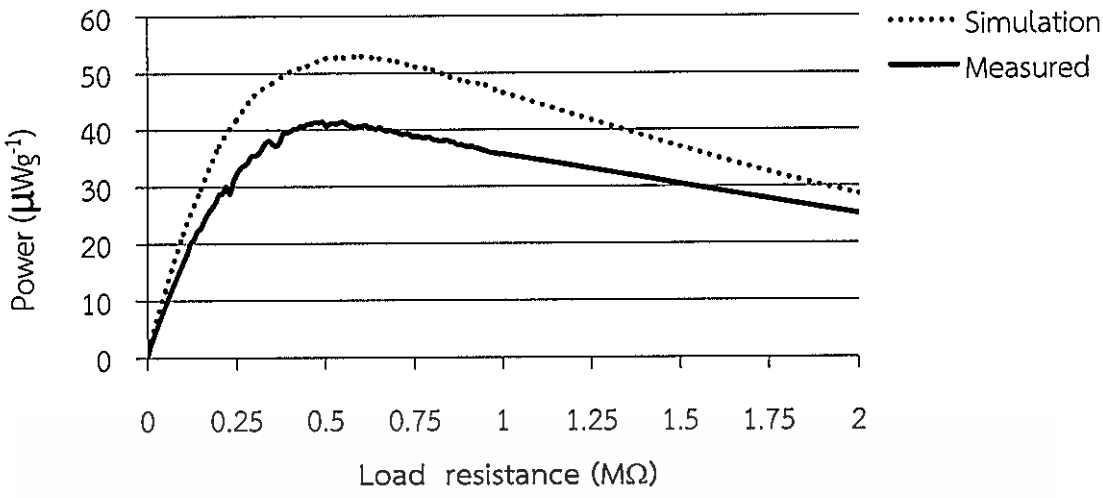

Figure 4.14 Power transfer to load resistors of the unimorph polycrystalline PZT piezoelectric energy harvester.

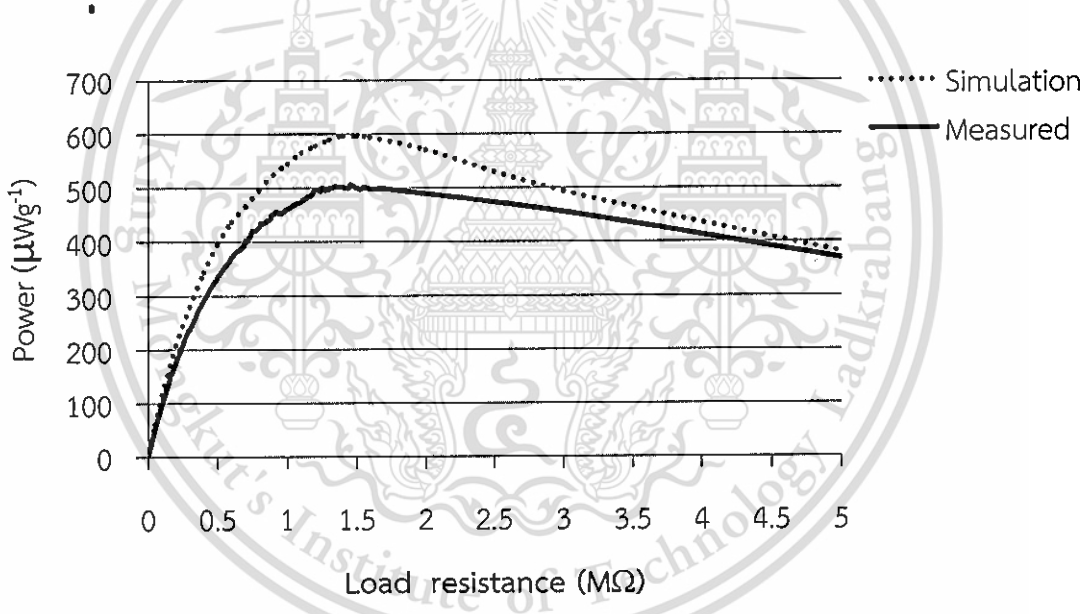

Figure 4.15 Power transfer to load resistors of the unimorph monocrystalline PMN-PT piezoelectric energy harvester.

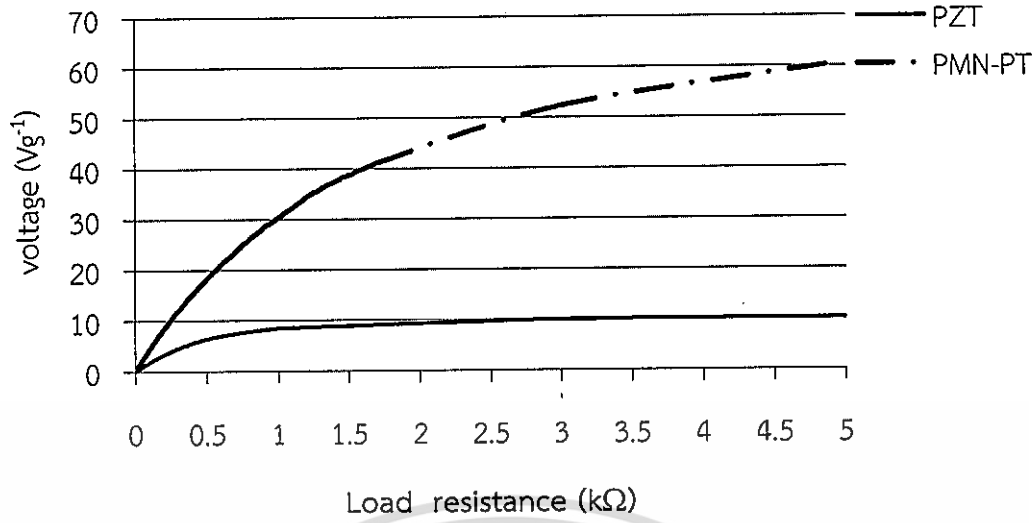

Figure 4.16 Voltage across load resistors of the unimorph polycrystalline PZT and monocrystalline PMN-PT piezoelectric energy harvesters.

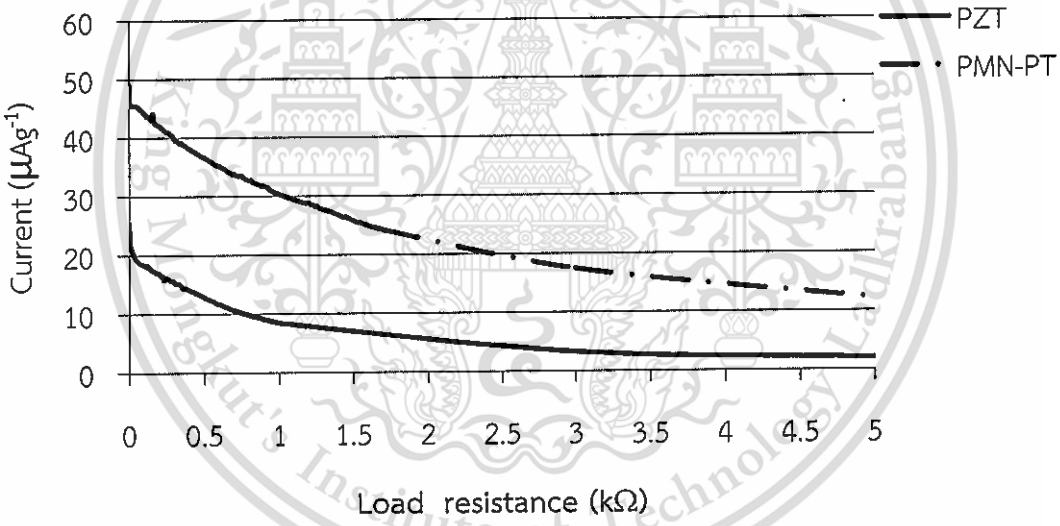

Figure 4.17 Current across resistors of the unimorph polycrystalline PZT and monocrystalline PMN-PT piezoelectric energy harvester.

Most of the important parameters for comparison of the unimorph polycrystalline PZT and single-crystalline PMN-PT piezoelectric energy harvesters were demonstrated in Table 4.5. The unimorph monocrystalline PMN-PT piezoelectric energy harvester gives the best performance.

Table 4.5 Performance comparison between piezoelectric polycrystalline PZT and monocrystalline PMN-PT unimorph energy harvesters

Performance Parameters	Polycrystalline PZT	Monocrystalline PMN-PT
Coupling Coefficient (k_{eff})	0.14	0.30
Everage Quality Factor (Q)	17.59	15.70
Capacitance (C_P)	1.75 nF	2.66 nF
Voltage (V)	31.56 Vg^{-1}	169.30 Vg^{-1}
Optimal Load Resistance (R_{opt})	0.49 M	1.25 M
Generated Power (P)	41.20 μWg^{-1}	500.07 μWg^{-1}

4.6 Conclusions

The study on the unimorph polycrystalline PZT and monocrystalline PMN-PT piezoelectric energy harvesters focusing on design and performance comparison were presented in this chapter. The designed models were optimized using finite element method (FEM). A comparative study of harvesters were done following the parameters of electromechanical coupling coefficient, quality factor, capacitance, generated voltage, and generated power at optimal load resistor. The performance comparison illustrates that, the unimorph monocrystalline PMN-PT piezoelectric energy harvester is an optimal device with greater performance.

Chapter 5
Piezoelectric Energy Harvesting from Machine Vibrations for Wireless Sensor System

5.1 Vibration Source

In order to generate the maximum power in resonant type energy harvester, the resonant frequency of the piezoelectric cantilever must match the frequency of the vibration source. Therefore, the amplitudes and frequencies of vibration source are the basic information for the energy harvester device design. The purpose of this chapter is to fabricate the energy harvester for powering a wireless sensor node in the Fully Automatic Dicing Saw machine (SINGULATION MODEL: DFD 6340). To estimate the energy source, an accelerometer (EI-CALC) was used to characterize the harvestable vibration. Due to examination of energy source, the harvestable vibrations come from a spinning and rising system. An idea about the integration of piezoelectric energy harvester and vibration source is shown in Figure 5.1.

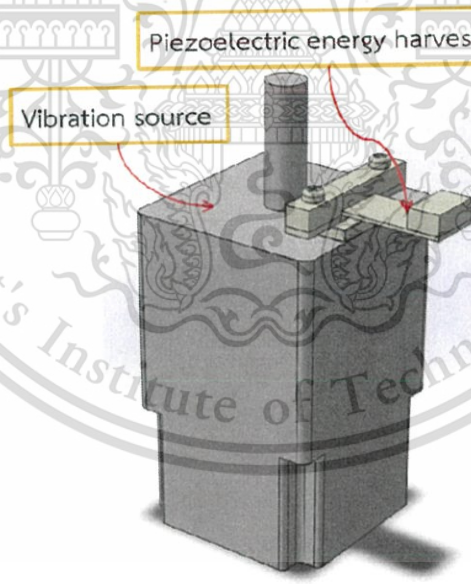

Figure 5.1 A schematic diagram of vibration source and piezoelectric energy harvester

The measured results in Figure 5.2 are given from the vibration measurement of accelerometer (EI-CALC). It was shown in time domain and frequency domain. Since the

energy harvesters exciting at low resonant frequency can generate the high power generation due to a large mass in the tip of cantilever [33]. Therefore, the three harmonic frequencies locating at 25, 50 and 75 Hz with acceleration aptitude 3.53, 0.56 and 1.53 m/s^2, respectively, are the most interesting parameters for contributing in the harvesters design.

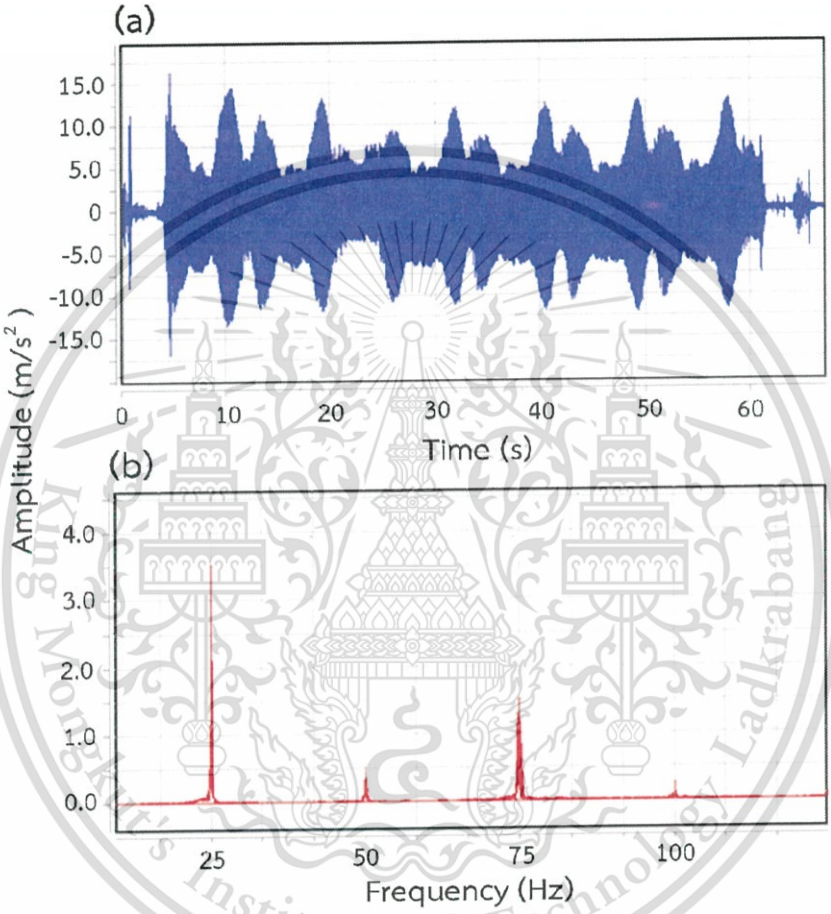

Figure 5.2 (a) Time domain and (b) frequency domain of the vibration source.

5.2 Concept Design

In Figure 5.3, the design of energy harvester was base on bimorph configuration. A piezoelectric bimorph cantilever was made from a two layer sheet of PZT material (PSI-5A4E) with a steel center shim as shown in Figure 5.4. Its total size is 12.7 x 31.8 x 0.51 mm^3; A commercial product from "Piezo System, Inc.". Instead of soldering wires to piezoelectric, the base of piezoelectric cantilever is squeezed by the PCB and acrylic to

simplify the cantilever range adjustment. A tungsten mass is placed at the free end for tuning resonant frequency.

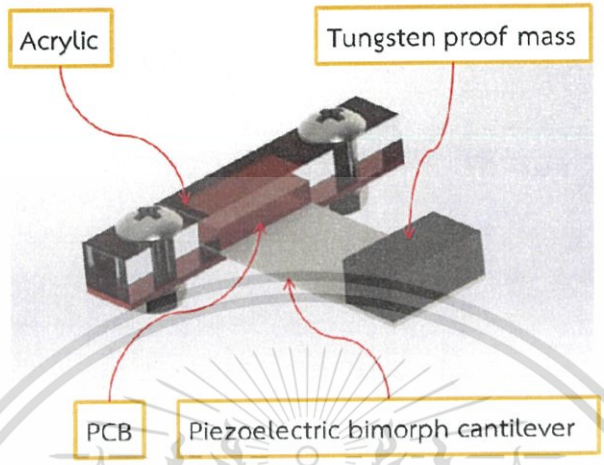

Figure 5.3 Model of energy harvesting device

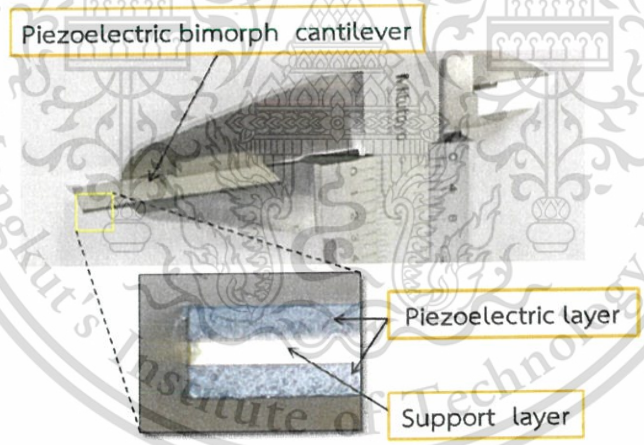

Figure 5.4 Piezoelectric bimorph cantilever

- Harvesters configuration

According to the consideration of vibration source, the energy harvesting devices operating at resonant frequency 25, 50, and 75 Hz are the purpose of design. To predict the dimension of harvesters, the Finite Element (FE) modeling was performed with modal analysis using the commercial software ANSYS 14.0. In implementation, a base of

contriver was clamped for 5 mm, and a tungsten mass was placed at the free end of cantilever in order to tune the resonant frequency. Table 5.1 shows the simulated weight and volume of masses, and resonant frequencies of numerical models. As the simulation results, a piezoelectric generator exciting at resonant frequency 25 Hz risk to crack during experiment because it accommodates a heavy mass under the highest acceleration. Generally, the generator exciting at constant acceleration with lower frequency [33] or constant frequency with higher acceleration will be able to generate the higher power. In this case, a harvester exciting at lower frequency 50 Hz is inputted a lower acceleration by the vibration source, and conversely a harvester with resonant frequency 75 Hz receives the higher acceleration. So, both of them are very interesting to consider their harvestable energy.

Table 5.1 Simulated frequencies, and weight and volume of mass

Frequency of Cantilevers (Hz)	Weight of Proof Mass (g)	Mass Volume (Width x Length x Thickness) mm^3
24.775	88.2	15 x 40 x 7.5
49.865	18.7	9 x 12.7x 8.35
74.913	11.761	6.3 x 12.7 x 7.5

5.3 Prototype of Harvesters

As the discussion of numerical models, two piezoelectric generators having different resonant frequencies of 50 Hz and 75 Hz were fabricated as demonstrated in Figure 5.5. In order to complete the served energy harvesting devices, their resonant frequencies were examined using the electro-mechanical impedance technique [34]. A piezoelectric energy harvester is connected in series with a 100 kΩ resistor and a function generator. 1 V from a function generator was supplied to a circuit as shown Figure 5.6. While sweeping the frequency on function generator, the voltages across energy harvester and reference resistor are measured for calculating the impedance of harvester. In a series circuit, all of the components carry the same current. Therefore, the impedance occurring in energy harvester can be found using following an equation

$$Z = \frac{V_{Piezo} R}{V_R} \tag{5.1}$$

where, Z is the impedance of piezoelectric energy harvester, V_{Piezo} is the voltage across piezoelectric energy harvester, R is resistance and V_R is the voltage across resistor.

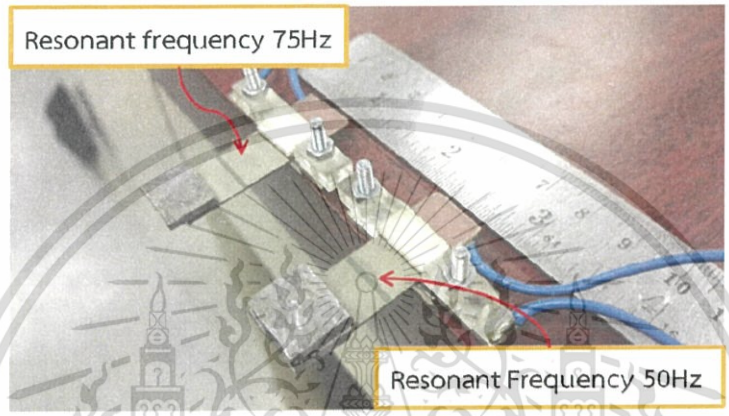

Figure 5.5 Piezoelectric energy harvesters.

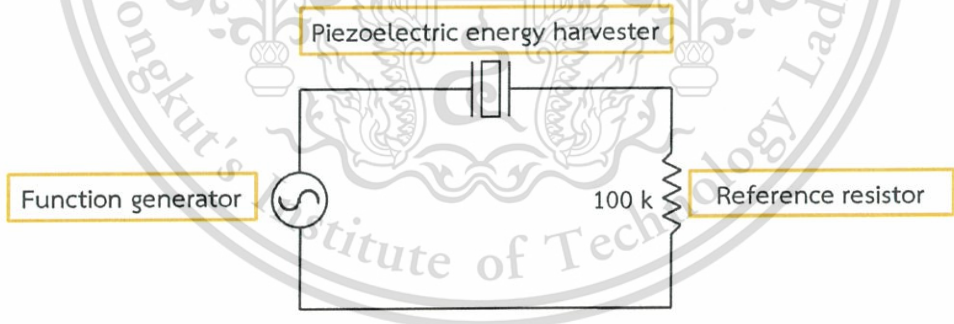

Figure 5.6 The measurement of resonant frequency of harvesters.

The results of impedance measurements are illustrated in Figure 5.7 and 5.8. The resonant frequency of harvesters approximately equal 50 and 75 Hz, which are the good results; a peak point with maximum impedance in a graph is the anti-resonant frequency and a lowest point with minimum impedance is the resonant frequency.

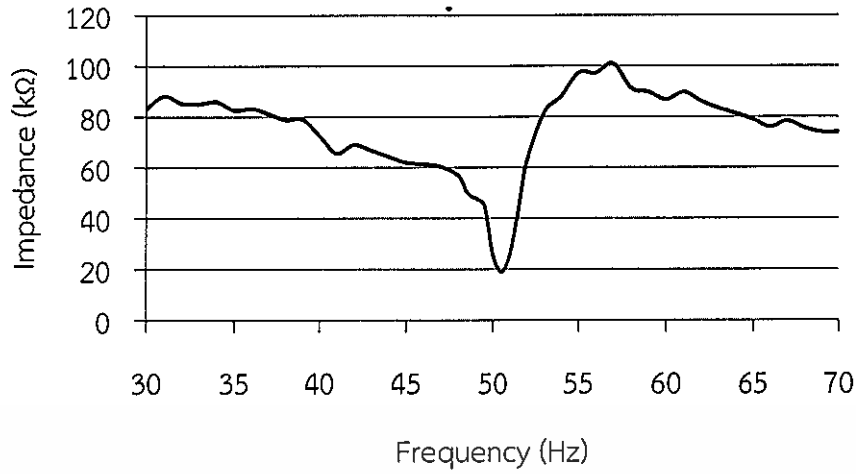

Figure 5.7 The impedance Vs. frequency of 50 Hz resonant device.

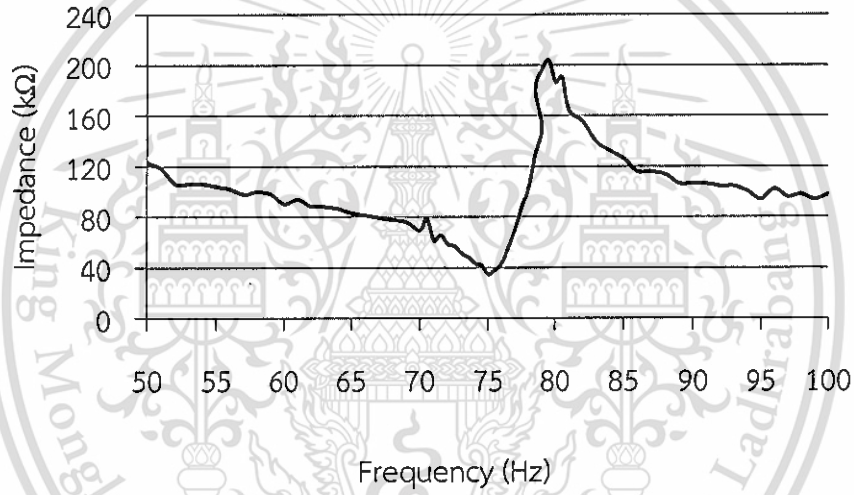

Figure 5.8 The impedance Vs. frequency of 75 Hz resonant device.

5.4 Energy Harvesting Experiment and Discussion

For the experiment of harvesting energy, two fabricated harvesters were mounted to the spinning and rinsing system. While the system is running, an energy harvester operating at its resonant frequency 50 Hz is able to generate the output voltage higher than a 75 Hz device as 29.2 V and 20 V in Figure 5.9 and 5.10, respectively. As consequence of this, a device with 50 Hz resonant frequency is more appropriate to consider as the power source of wireless sensor node.

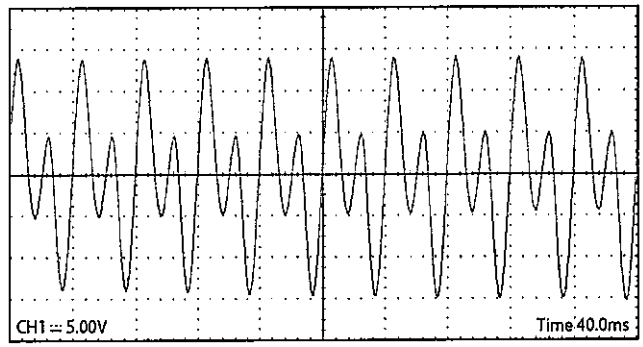

Figure 5.9 Generated voltage from an energy harvester exciting at its resonant frequency 50Hz

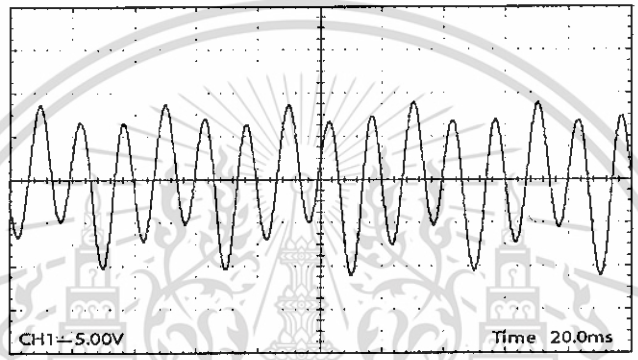

Figure 5.10 Generated voltage from an energy harvester exciting at its resonant frequency 75 Hz

Because the wireless sensor consumes DC voltage with constant power, therefore, the energy management circuit (LTC3588-1) is used to rectify the output voltage of piezoelectric harvester into usable DC voltage as shown in Figure 5.11. In the experiment, the generated power was transferred to charge a 2200 μF capacitor [35]; it was utilized to store the harvestable energy for supplying to wireless sensor node through the buck converter. The wireless sensor node consumes the average power 44.31 μW in the operation time 300.03 seconds or around 13.29 mJ. The operative voltage range of the LTC3588-1 is 3.6V-5V.

The Figure 5.12 shows the time period of charging a 2200 μF capacitor from 0 V to 5 V (threshold voltage). The energy charging to capacitor is discrete due to the operation time of a spinning and rinsing system. It runs 60 seconds and stops about 180–600 seconds before coming to run again. The spaces in graphs occurred by taking off the oscilloscope probe during paused system in order to prevent the current leakage. The

discharged state came from the current consumption of components in energy management circuit (Quiescent Current), The energy harvesting conditions were considered on the shortest and longest time of the system stop as 180 seconds and 600 seconds, where the time period of charging capacitor is 2507 seconds and 8358 seconds, respectively. In this case, the stored energy in the capacitor can be calculated by

$$E_C = \frac{1}{2}CV^2 \tag{5.2}$$

where, E_C is the energy stored in a capacitor, C is the capacitance and V is the voltage across capacitor. When the voltage across capacitor reaches to the threshold, the stored energy is around 27.50 mJ, which is enough for the wireless sensor node [25].

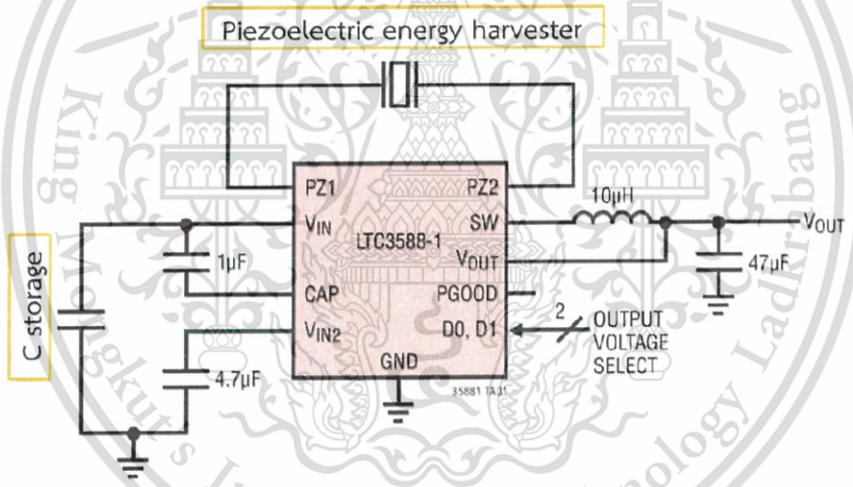

Figure 5.11 Energy management circuit.

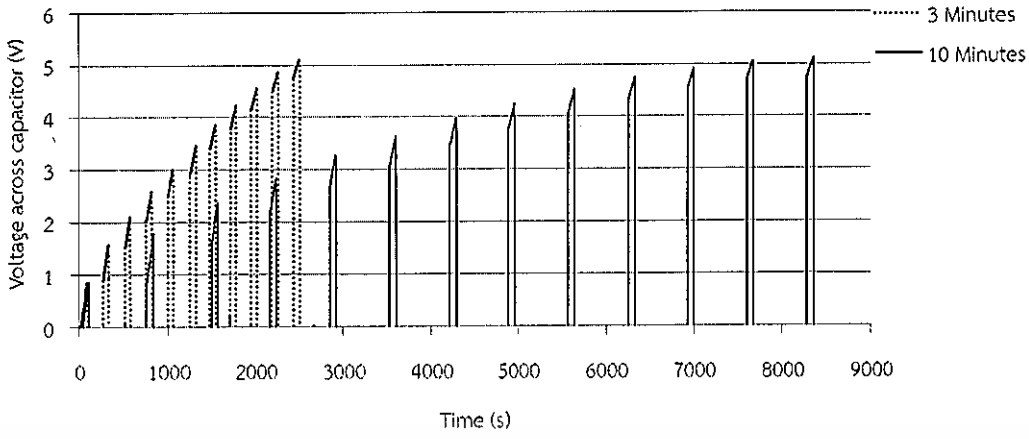

Figure 5.12 Voltages across a capacitor Vs. charging time.

5.5 Conclusions

In this chapter, the resonant frequency of piezoelectric energy harvesters was designed to match the frequency of vibration source in order to achieve the maximum power generation. The Finite Element Method (FEM) was utilized to analyze the natural frequency of designed models. By following the simulation results and conditional vibration of machine, two designed harvesters operating at 50 and 75 resonant frequency were fabricated and then considered their generated voltage. As the experiment result, a harvester with its resonant frequency 50 Hz was able to generate the higher voltage. The generated energy was stored in a 2200 μF capacitor through the energy management circuit (LTC3588-1), which is enough for wireless sensor node when the voltage across a capacitor reaches to the threshold.

Chapter 6
Conclusions

6.1 Summary

This thesis has presented the comparative study of unimorph piezoelectric energy harvesters based on polycrystalline PZT and monocrystalline PMN-PT materials, and the study of bimorph piezoelectric energy harvesting from machine vibration for powering the wireless sensor node. The unimorph piezoelectric energy harvesters were assumed to excite at resonant frequency of 150 Hz due to the frequency of many vibration sources (60-200Hz) for energy harvesting experiment. The assumed frequencies and acceleration levels from electromagnetic shaker is not high accuracy, since the vibration source was controlled using open-loop controllers and monitored using accelerometer. The parameters of electromechanical coupling coefficient, quality factor, capacitance, generated voltage and output power were considered to compare the energy harvesting performance of unimorph piezoelectric energy harvesters. As can be seen, the unimorph monocrystalline PMN-PT piezoelectric energy harvester outperforms the unimorph polycrystalline PZT piezoelectric energy harvester in terms of the overall capability of voltage, current and power generation.

According to the vibration source conditions from a spinning and rinsing system of the Fully Automatic Dicing Saw machine, the bimorph polycrystalline PZT piezoelectric energy harvesters having resonant frequency of 50 and 70 Hz were fabricated to harvest the vibration energy. From the experimental results, a harvester exciting at its resonant frequency 50 Hz was able to generate the higher output voltage, which was used on further test with the energy management circuit for storing the generated energy at capacitor. While a spinning and rising system stop or no energy from harvester, the stored energy in capacitor was discharged. It causes a long period of time for charging capacitor. However, the stored energy is enough to supply as the energy consumption of wireless sensor node.

REFERENCES

[1] V. C. Gungor and G. P. Hancke, "Industrial Wireless Sensor Networks : Challenges, Design Principles, and Technical Approaches," *IEEE Trans. Ind. Electron.*, Vol. 56, No. 10, pp. 4258–4265, October 2009.

[2] Yen Kheng Tan and Sanjib Kumar Panda, "Energy Harvesting From Hybrid Indoor Ambient Light and Thermal Energy Sources for Enhanced Performance of Wireless Sensor Nodes," *IEEE TRANSACTIONS ON INDUSTRIAL ELECTRONICS,* Vol. 58, No. 9, pp. 4424–4435, September 2011.

[3] Paul D. Mitcheson and el at, "Energy Harvesting From Human and MachineMotion for Wireless Electronic Devices," *Proceeding of the IEEE*, Vol.96, No.9, pp. 1457-1486, 2008.

[4] Jianmin Hou and Yi Gao, "Greenhouse Wireless Sensor Network Monitoring System Design Based on Solar Energy," *2010 International Conference on Challenges in Environmental Science and Computer Engineering*, pp. 475-479, 2010.

[5] Vaclav Smil, Energy at the Crossroads, 2006, oecd.org

[6] R. J. M. Vullers, R. Van Schaijk, I. Doms, C. Van Hoof, and R. Mertens, "Micropower energy harvesting," *Solid-state Electron.*, vol. 53, pp. 684-693, 2009.

[7] S. P. Beeby, M. J. Tudor, and N. M. White, "Energy harvesting vibration souces for microsystem applications," *Meas. Sci. Technol.*, Vol. 17, pp. R175-R195, 2006.

[8] Hagerty J, Helmbrecht F, McCalpin W, Zane R, Popovi&cacute Z. Recycling "Ambient Microwave Energy with Broad-band Rectenna arrays." *IEEE Transactions on Microwave Theory and Techniques*, 2004.

[9] P. Glynne-Jones, M. J. Tudor, S. P. Beeby, and N. M. White, "An Electromagnetic, Vibration-powered Generator for Intelligent Sensor Systems," *Sens. Actuators*, A, Vol. 110, pp. 344-349, 2004.

[10] F. Peano and T. Tambosso, "Design and optimization of a MEMS electret-based capacitive energy scavenger," *J. Microelectromech. Syst.*, Vol. 14, pp. 435-529, 2005.

[11] D. Shen, S. –Y. Choe, and D. –J. Kim, "Analysis of Piezoelectric Materials for Energy Harvesting Devices under High-g Vibrations," *Jpn. J. Appl. Phys.*, Vol. 46, pp. 6755-6760.

[12] S. Roundy and P. K. Wright, "A Piezoelectric Vibration Based Generator for Wireless Electronics," *Smart Materials and Structures*, Vol. 13, pp. 1131-1142, 2004.

[13] C.B. Williams, and R.B. Yates, "Analysis of a Micro-electric Generator for Microsystems." *Sens. Actuators A, Phys.*, Vol. 52, pp. 8-11, 1996.

[14] S. Roundy, P.K. Wright, and J.M. Rabaey, "Energy Scavenging for Wireless Sensor Network." *Kluwer Academic Publisher*, Massachusetts, USA, 2004.

[15] Song H -C, Kim H -C, Kang C -Y, Kim H -J, Yoon S -J and Jeong D -Y "Multilayer Piezoelectric Energy Scavenger for Large Current Generation." *J. Electroceram.*, Vol. 23, pp. 301-304, 2009.

[16] T.M. Kamel, R. Elfrink, M. Renaud, D. Hohlfeld, M. Goedbloed, C. de Nooijer, M. Jambunathan, and R. van Schaijk, "Modeling and Characterization of MEMS-based Piezoelectric Harvesting Devices," *J. Micromech. Microeng.*, Vol. 20, No. 10, pp. 105023, 2010.

[17] N.G. Elvin, and A.A. Elvin, "A Coupled Finite Element-circuit Simulation Model for Analyzing Piezoelectric Energy Generators," *J. Intell. Mater. Syst. Struct.*, Vol. 20, pp. 587-595, 2009.

[18] M. Zhu, E. Worthington, and J. Njuguna, "Analyses of Power Output of Pezoelectric Energy Harvesting Devices Directly Connected to a Load Resistor using a Coupled Piezoelectric Circuit Finite Element Method," *IEEE Transaction on Ultrasonics, Ferroelectrics and Frequency Control*, Vol. 56, pp. 1309-1317, 2009.

[19] F .Lu, H.P. Lee, and S.P. Lim, "Modeling and Analysis of Micropiezoelectric Power Generators for Micro-electromechanical-systems Application," *Smart Mater. Struct.*, Vol.13, no. 1, pp. 57-63, 2004.

[20] X. Gao, "Vibration and flow energy harvesting using piezoelectric," *PhD dissertation, Drexel University*, 2011.

[21] Marauska S, Hrkac V, Dankwort T, Jahns R, Quenzer H J, Kn¨ochel R, Kienle L and Wagner B "Sputtered thin film piezoelectric aluminum nitride as a functional MEMS material," *Microsystem Technologies*, Vol. 18, pp. 787–95, 2012.

[22] Crisler D F, Cupal J J and Moore A R "Dielectric, piezoelectric, and electromechanical coupling constants of zinc oxide crystals," *Proc. IEEE*, Vol.56, pp. 225–226, 1968

[23] Priya, S. and D.J. Inman, "Energy harvesting Technologies," *New York: Springer,* 2009.

[24] IEEE standard of piezoelectricity, Standards Committee of the IEEE Ultrasonics, Ferroelectrics, and Frequency, *Control Society, USA*, pp. 176, 1988.

[25] Piefort, Finite Element Modeling of Piezoelectric Active Structures (doctoral thesis), *University of Brussels*, pp. 51–69, 2001.

[26] H. Allik, T. J. R. Hughes, "Finite element method for piezoelectric vibration," *International Journal for Numerical Methods in Engineering,* Vol. 2, pp. 151–157, 1970.

[27] G. L. C. M. de Abreu, J. F. Ribeiro, V. Steffen, "Finite element modelin gof a plate with localized piezoelectric sensors and actauators," *J. Of the Braz. Soc. Of Mech. Sci. & Eng*, Vol. 26 (2), pp. 117–128, 2004.

[28] D. Boucher, M. Lagier, C. Maerfeld, "Computation of the vibration modes for piezoelectric array transducers using a Mixed Finite Element-perturbation method," *IEEE Transactions on Sonds and Ultrasonic, SU, Vol.* 28 (5), pp. 318–330, 1981.

[29] Jiashi Yang, "An introduction to the theory of piezoelectricity," *Springer, Lincoln*, 2005.

[30] S. Roundy, P. K. Wright, and J. Rabaye, "A Study of Low Level Vibrations as a Power Source for Wireless Sensor Nodes," *Computer Communications*, Vol. 26, pp. 1131-1144, 2003.

[31] K.C. Kim, Y.S. Kim, H.J. Kim, S.H. Kim "Finite Element Analysis of Piezoelectric Actuator with PMN–PT Single Crystals for Nanopositioning," *Current Applied Physics*, Vol. 6, pp. 1064–1067, October 2006.

[32] D. Shen, J.-H. Park, J. Ajitsaria, S.-Y. Choe, H.C. Wikle III, D.-J. Kim, "The Design, Fabrication and Evaluation of a MEMS PZT Cantilever with an Integrated Si Proof Mass for Vibration Energy Harvesting," *J. Micromech. Microeng.*, Vol. 18, No. 5, Article No. 055017, 2008.

[33] E.E. Aktakka, L.P. Rebecca, and K. Najafi "Thinned-PZT in SOI process and design optimization for piezoelectric inertial energy harvesting," *in Proc. 16th Int. Conf.Transducers'11*, June 5-9, 2011, Beijing, China, pp. 1649-1652.

[34] Suresh Bhalla, Ashok Gupta, Sahll Bansal and Tarun Garg, "Ultra Low-cost Adaptations of Electro-mechanical Impedance Technique for Structural Health Monitoring," *Journal of Intelligent Material Systems and Structures*, Vol.20, pp. 991-999, 2009.

[35] Don Isarakorn, Thapanun Sudhawiyangkul and Songmoung Nundrakwang, "Energy Analysis in Zigbee based Wireless Sensor Node Powered by Piezoelectric Energy Harveste", *Advanced Materials Research*, Vols. 931-932, pp. 1328-1332, 2014.

APPENDIX A
List of Publications

International Conferences

[1] **Phosy Panthongsy**, Don Isarakorn, Thapanun Sudhawiyangkul, Songmoung Nandrakwang "Piezoelectric Energy Harvester from Machine Vibrations for Wireless Sensor System." **International Conference on Electrical Engineering/Electronics, Computer, Telecommunications and Information Technology, ECTI-CON 2015, Hua Hin, Thailand,** 24-27 June 2015, pp. 1-6.

[2] **Phosy Panthongsy**, Don Isarakorn "Comparative Study of Piezoelectric Energy Harvesters Based on Polycrystalline PZT and Single-crystalline PMN-PT Materials." **International Conference on Electrical Engineering/Electronics, Computer, Telecommunications and Information Technology, ECTI-CON 2016, Chiang Mai, Thailand,** 28 June 2016 - 1 July 2016, pp. 1-5.

Piezoelectric Energy Harvesting from Machine Vibrations for Wireless Sensor System

Phosy Panthongsy
International College
King Mongkut's Institute of Technology Ladkrabang
Bangkok 10520, Thailand

Don Isarakorn, Thapanun Sudhawiyangkul
and Songmoung Nundrakwang
Department of Instrumentation and Control Engineering,
Faculty of Engineering
King Mongkut's Institute of Technology Ladkrabang
Bangkok 10520, Thailand
kidon@kmitl.ac.th

***Abstract*— In recent years, wireless sensor network is used in a variety of applications and highly required. These wireless sensor network is powered by the battery with limit energy. Therefore, the integration of energy harvester and wireless sensor network has received more attention because it can prolong the lifetime of battery in a sensor node. The focus of this paper is to design the energy harvesting device from machine vibrations for wireless sensor node, which the amplitude and frequency of vibration source were contributed on the design. The structure of energy harvesting devices is a resonant type piezoelectric energy harvester with a proof mass at the tip of the beam for tuning its resonant frequency. The proposed piezoelectric energy harvesters were then designed and analyzed by using Finite Element Method (FEM) to optimize the natural frequency of the harvester. Then, the prototype energy harvesters were made and mounted to a vibration source for experiments. The result reveals that the optimal piezoelectric energy harvester can generate the output power of 82.29 μW at the resonant frequency of 50 Hz.**

Keywords—Piezoelectric transduction; Machine vibrations; Energy harvesting

I. INTRODUCTION

In over years, wireless sensor network is widely used in various fields of works whether in industry or agriculture. Due to its flexibility of communication without wiring, many wireless sensors are usually designed to run on batteries [1]. However, when the sensor is on the situation of tracing the important information in harsh and inaccessible environment, the replacement of depleted batteries becomes unfavorable, so that, alternative methods for powering wireless sensor nodes are required. Therefore, the energy harvesting from ambient environment is being given more attention from various researchers because of its undepletable energy can be used to replace or prolong the life of battery in the sensor node. The available primary energy sources that can be harvested and integrated into the sensor node are solar energy [2], thermal energy [3], mechanical energy [4] and energy from electromagnetic waves (RF) [5]. From these energy resources, the mechanical vibrations are very attracted as a potential source of power for wireless sensor in the industrial factory because the machines using to conduct the production usually make the vibration when operating. There are three kinds of transduction methods for harvesting vibration energy; electromagnetic [6], electrostatic [7], and piezoelectric conversions [8].

Among three kinds of transducers, a piezoelectric generator has the maximum power density [9] and it can be significantly divided into two types; impact type and resonant type. The impact type harvester operates without concerning about resonant frequency and is used in impact excitation environment. On the other hand, resonant type harvester is a type that needs to be exited at its resonant frequency in order to obtain the maximum displacement leading to the maximum power generation; this is feasible by tuning the harvester natural frequency to match the source frequency [9]. Therefore, the piezoelectric harvester is the most interesting device for harvesting energy from mechanical vibration [10-12] due to its conversion efficiency with simple structure and mass manufacturability.

The purpose of this paper is to design and realize the piezoelectric energy harvester with matching resonant frequency that can provide enough power to the sensor node [13]. The vibration source was investigated for generating the numerical model of piezoelectric beam. Different aspects related to energy harvester design, optimization and electrical characteristic are demonstrated. Also the prototype harvesters are made and tested with the spinning and rinsing system of the fully automatic dicing saw machine (SINGULATION MODEL: DFD 6340) for energy harvesting.

II. VIBRATION SOURCE FOR ENERGY HARVESTING

In order to generate the maximum power in resonant type energy harvester, the resonant frequency of the piezoelectric cantilever must match the frequency of the vibration source. Therefore, the amplitude and frequency of vibration source are the basic necessary information to design the energy harvester device. For this experiment of harvesting energy, an acceleration sensor (EI-CALC) was used to measure the vibration source, which occurs from spinning and rinsing system of the fully automatic dicing saw machine (SINGULATION MODEL: DFD 6340) located as shows in Fig 1.

AUN/SEED-Net, JICA

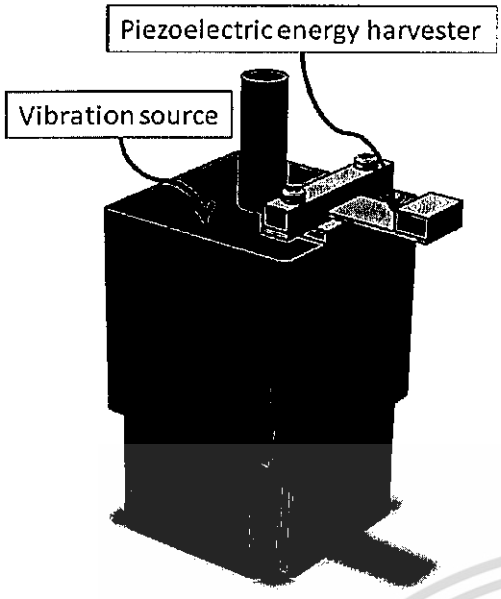

Fig. 1. A schematic diagram of vibration source and piezoelectric energy harveester.

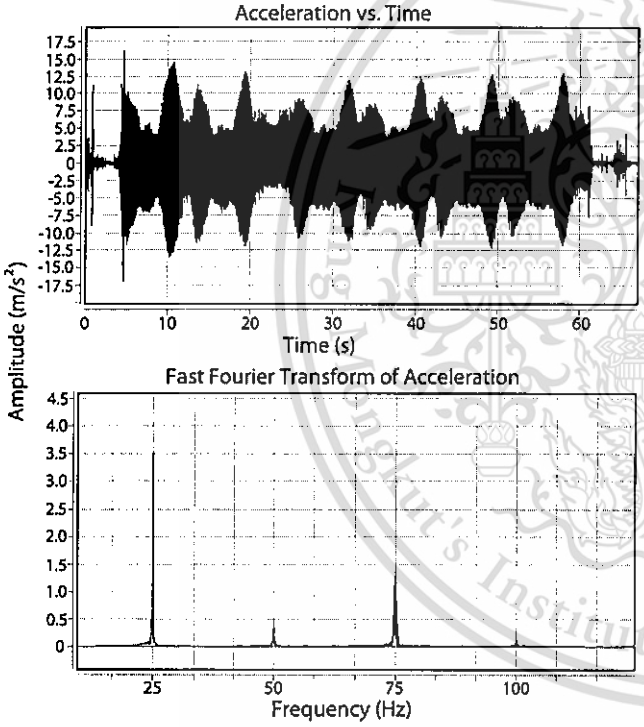

Fig. 2. The acceleration profile and its Fast Fourier Transform (FFT) of the vibration source.

When the vibration data from the accelerometer is transformed from the time domain to the frequency domain, three harmonic frequencies shown in Fig. 2 are located at 25, 50 and 75 Hz, which, have amplitude values of up to 3533, 560 and 1535 mm/s^2, respectively. These data is necessarily used as the parameters for the harvester design.

III. Design of Vibration Energy Harvester Model

A numerical model of the energy harvester device is essential for estimating the natural frequency and amount of the power generated by piezoelectric transduction. A size of PSI-5A4E piezoelectric cantilever (Piezo System, Inc.) used to design the energy harvester is 12.7 mm x 31.8 mm x 0.51 mm. The model utilized in this work is based on applied resonant type piezoelectric energy harvester in [9] as shown in Fig. 3. Instead of soldering wires to piezoelectric, the base of piezoelectric cantilever is squeezed by the PCB and acrylic to simplify cantilever range tuning.

A. Natural frequency of piezoelectric cantilever

For the piezoelectric energy harvester in resonant type, the natural frequency of cantilever structure is important. In order to get a maximum value of power, the resonant frequency of piezoelectric cantilever has to be tuned to match the harmonic frequency of vibration source. Hence, the simulation is carried out using ANSYS to create Finite Element Model and determine the natural frequencies of the energy harvesting devices.

To tune the resonant frequency of the cantilever, mass of tungsten is placed at the free end of the beam. Table1 shows the weight, size and the simulated resonant frequency of the model. At 25 Hz resonant frequency from Table1, the size of mass is considered large compare to the size of the beam, while the cantilevers with 50 and 75 Hz are more appropriate option due to their smaller size.

B. Simulation of energy harvesting

For any piezoelectric cantilevers with the same dimension, the displacement of the cantilever's tip is directly proportional to the output power. Therefore, comparing the displacement can demonstrate the optimal size of mass at the tip of piezoelectric beam. To examine the vertical displacement, two cantilever models with different resonant frequencies of 50 and 75 Hz are simulated in harmonic analysis. A force of 10 μN with damping ratio 0.1% is applied to the tip of the beam for producing vibration. Fig. 4 shows the vertical displacements of beams as 30 μm and 26 μm, respectively.

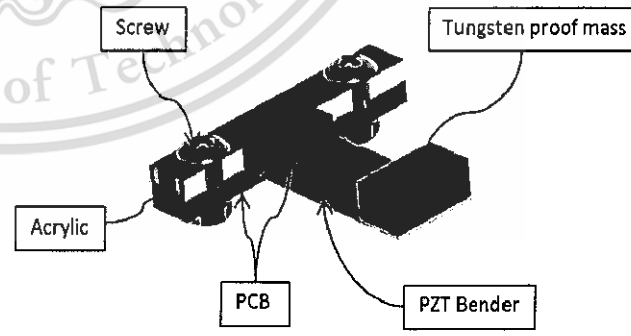

Fig. 3. Structure model of energy harvesting device.

TABLE I. RESULT OF MODEL SIMULATION

Frequency of cantilever (Hz)	Weight of proof mass (g)	Size of mass (Width x Length x Thickness) (mm^3)
24.775	88.2	15 x 40 x 7.5
49.865	18.7	9 x 12.7x 8.35
74.913	11.761	6.3 x 12.7 x 7.5

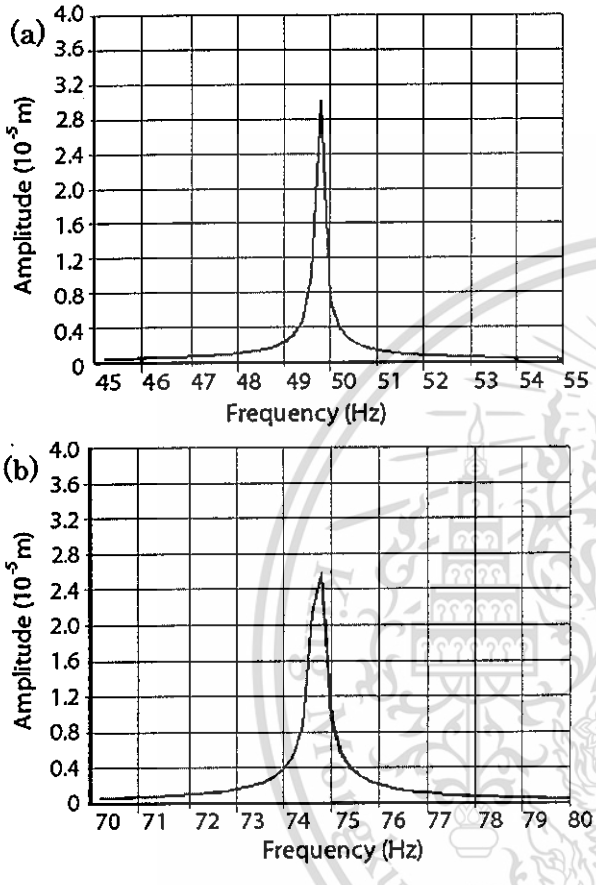

Fig. 4. Experimental results of the vertical displacement at the excitation in resonant frquencies at a) 50 Hz and b) 75 Hz.

In order to get maximum peak to peak voltage, static analysis is carried out at 50 Hz and 75 Hz for vertical displacement 30 μm and 26 μm, respectively. The displacement was then used as a parameter for the simulation. Two maximum output voltages were obtained at 12.66 V and 7.63 V as shown in Fig. 5 and 6, respectively.

IV. PROTOTYPE ENERGY HARVESTING DEVICE EXPERIMENT

From the numerical models of energy harvester, two piezoelectric generators having different resonant frequencies of 50 Hz and 75 Hz were fabricated for harvesting energy as shown in Fig. 7.

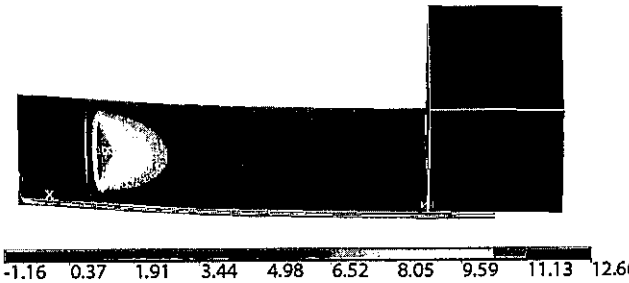

Fig. 5. The voltage distribution of cantilever resonating at 50 Hz.

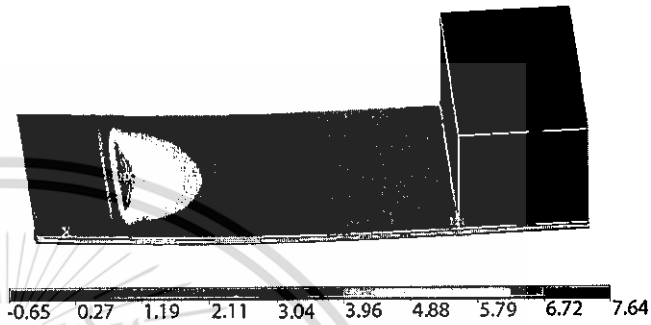

Fig. 6. The voltage distribution of cantilever resonating at 75 Hz.

The resonant frequencies of the piezoelectric energy harvesters were measured using the electro-mechanical impedance technique [14]. A piezoelectric energy harvester is connected in series with a 100kΩ resistor and a function generator. 1 V from a function generator was supplied to a circuit as shown in Fig.8. By sweeping the frequency on function generator, the voltages across energy harvester and resistor can be measured. The impedance of energy harvester was found using following equation:

$$Z = \frac{V_{PZT} R}{V_R} \quad (1)$$

Where, Z is the impedance of piezoelectric energy harvester, VPZT is the voltage across piezoelectric energy harvester, R is resistance and VR is the voltage across resistor.

From the experimental results of resonant frequencies measurements in Fig. 9 and 10, the peak point with maximum impedance in the graphs is the anti-resonant frequency and the lowest point with minimum impedance is the resonant frequency.

A. Energy harvesting output and energy management

For the experiment of harvesting energy, two piezoelectric energy harvesters were attached to the spinning and rinsing system. Fig. 11 and 12 show the output voltages of harvesters (50 and 75 Hz resonant model) when shaken by the vibration -

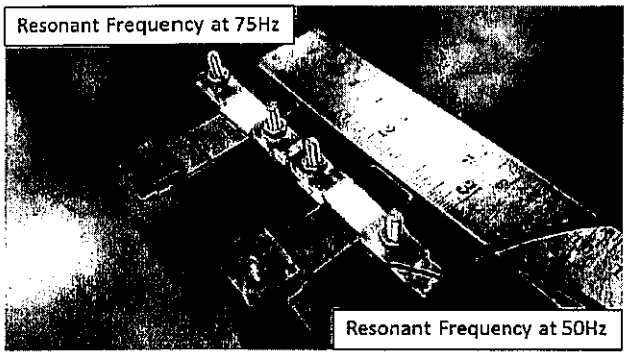

Fig. 7. Piezoelectric energy harvesters.

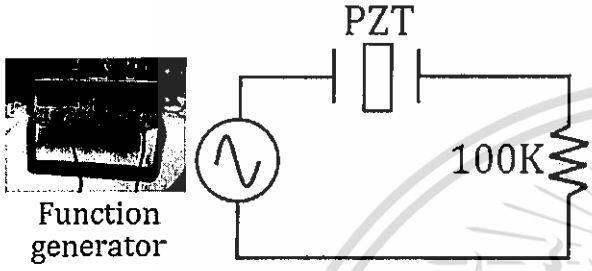

Fig. 8. Experimental setup for measuring the resonant frequecy of piezoelectric energy harvester.

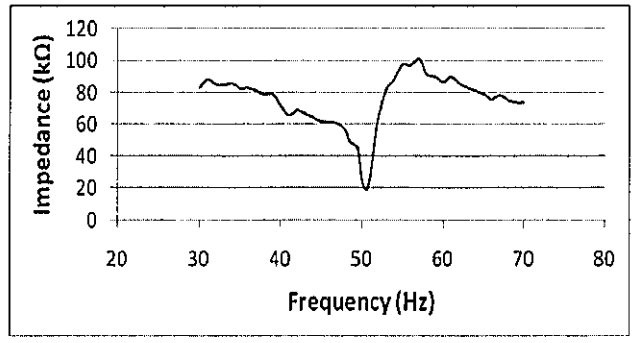

Fig. 9. The impedance vs frequency of 50 Hz resonant device.

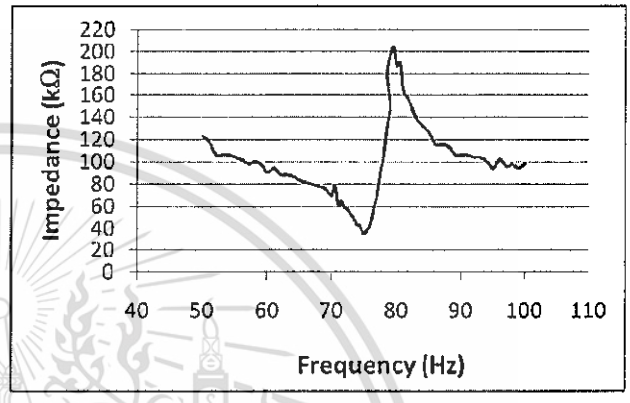

Fig. 10. The impedance vs frequency of 75 Hz resonant device.

of motor. The peak to peak voltages are 29.2 V and 20 V, respectively. From the results, the energy harvesting device exciting at its resonant frequency of 50 Hz is capable of generating higher voltage. Therefore, it is used for harvesting energy in further experiment.

Since the output voltage is alternative current with inconstant power, while the wireless sensor requires DC voltage with constant power as its power source. Therefore, the Energy Management Circuit (LTC3588-1) is used to rectify the output voltage of piezoelectric into usable DC voltage as shown in Fig. 13.

In this experiment, the AC output voltage of the energy harvester is conversed to DC voltage by energy management circuit LTC3588-1 for charging 2200 μF capacitor. When the spinning and rinsing system is operated, the result of output voltage measured across the capacitor is shown in Fig. 14. The maximum voltage is 6.7 V. In this case, the energy harvested from energy harvesting device can be found by using the formula that applied to calculate the electrical energy in the capacitor as:

$$E_c = \frac{1}{2} C V^2 \qquad (2)$$

Where, E_c is the energy stored in a capacitor, C is the capacitance and V is the voltage across capacitor.

A graph in Fig. 14 shows the voltage across capacitor in charging and discharging state. Charging state means during the spinning and rinsing system is working and generating the vibration, which electrical energy is harvested to accumulate into a capacitor. The discharging state occurs when the motor is stop running and has no vibration. The energy harvesting device is unable to harvest energy, and also electronic devices consume the electrical energy in normal (Quiescent Current). A power management circuit and capacitor also has the current leakage as well. Some of the current is leaked into oscilloscope probe with its impedance of 1 MΩ.

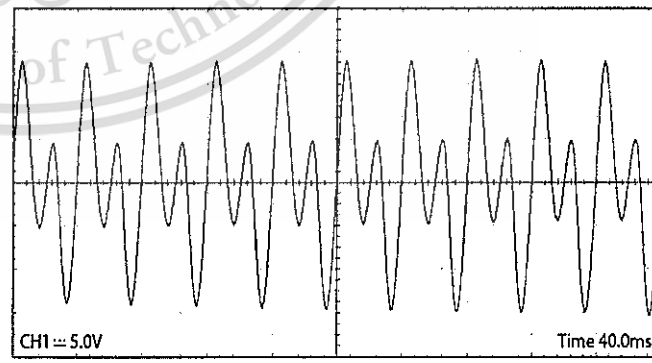

Fig. 11. Output voltage signal from 50 Hz resonant energy harvester.

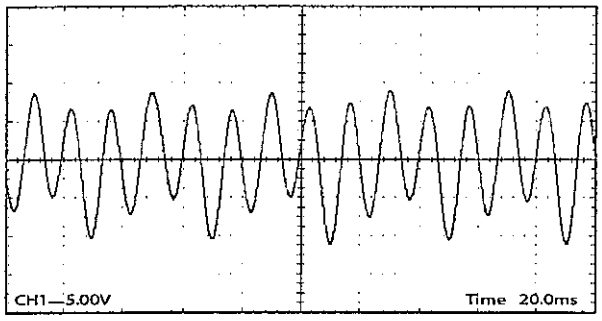

Fig. 12. Output voltage signal from 75 Hz resonant energy harvester.

For the experiment of energy storage, a 2200 μF capacitor is used to accumulate the energy from the harvester. Once the voltage across capacitor reach the threshold voltage (around 5.1V) of IC LTC3588-1, the energy in capacitor will be discharged though the buck converter to supply the energy to load

A graph in Fig. 15 shows the time period of charging 2200 μF capacitor from 0 V to 5.1 V. Since the spinning and rinsing system is not working all the times, it can be seen that the power charging into the capacitor is discrete. The system runs about 60 seconds for spinning and rinsing a wafer before waiting around 3 – 10 minutes to complete a sawing process. The period of sawing wafer is up to the sizes of wafer thus it is non perpetual. If the shortest time for wafer cutting is 3 minutes, the capacitor is charged for 45 minutes to reach the threshold voltage. If the longest time for wafer cutting is 10 minutes, the capacitor is charged for 145 minutes to reach the threshold voltage.

The observational results of energy harvested were compared as shown in Fig. 16. The piezoelectric energy harvester with 50 Hz resonant frequency can provide higher power (82.29 μW), while the 75 Hz resonant frequency harvester can generate 21.19 μW. Therefore, the generator vibrated at its resonant frequency of 50 Hz is more appropriate to integrate into a wireless sensor node, which requires the power of 44.31 μW [13].

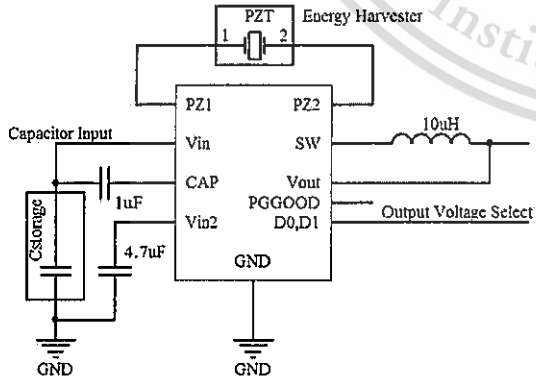

Fig. 13. Energy management circuit.

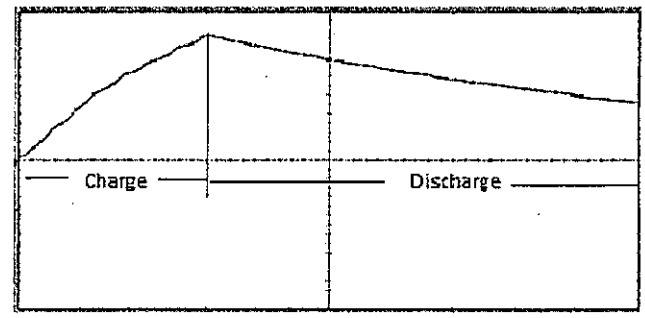

Fig. 14. Voltage measured across the capacitor.

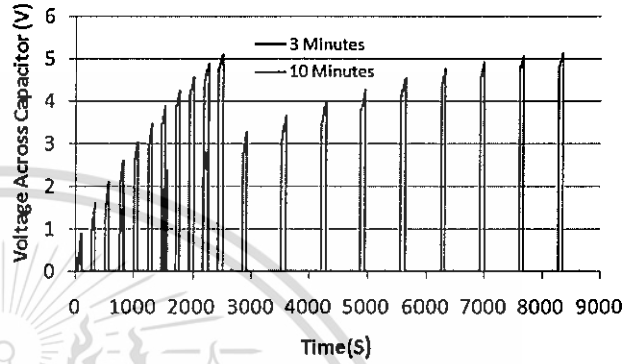

Fig. 15. Voltages measured across capacitors during the operation.

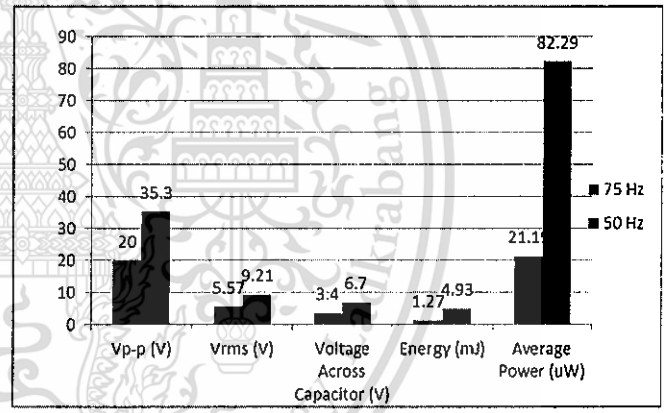

Fig. 16. Performance comparison of energy harvesting devices.

CONCLUSIONS

In this paper, the piezoelectric energy harvesters were designed to match the resonant frequency vibration. FEM was utilized to analyze the natural frequency and considered the optimal models. In order to maximize the beam's tip displacement and resonant frequency, the size of mass at the tip of cantilever are investigated. The proof masses of 88.2, 18.7 and 11.761 g were placed on tip of cantilevers in order to get resonant frequencies at 25, 50 and 75 Hz, respectively. The simulation results show that the harvester with 50 Hz resonant frequency is the most appropriate approach due to its size and output power compared to the others. Then, the prototype energy harvester with 50 Hz resonant frequency was made to use in the field test with the spinning and rinsing system. The

energy management circuit LTC3588-1 was used to convert the harvested energy from the harvester to usable energy. The experiment results reveal that the harvester can provide peak to peak voltage of 29.2 V and power up to 82.29 μW. the proposed harvester can be used as a power source for the sensor nodes [13].

ACKNOWLEDGMENTS

Phosy Panthongsy gratefully acknowledges the AUN/SEED-Net for the fully financial support in his postgraduate education and thanks King Mongkut's Institute of Technology Ladkrabang (KMITL), Bangkok, Thailand for providing the excellent research facilities.

REFERENCES

[1] V. C. Gungor and G. P. Hancke, "Industrial wireless sensor networks:Challenges, design principles, and technical approaches," IEEE Trans. Ind. Electron., vol. 56, no. 10, pp. 4258–4265, Oct. 2009

[2] Vaclav Smil, Energy at the Crossroads, 2006, oecd.org

[3] R. J. M. Vullers, R. Van Schaijk, I. Doms, C. Van Hoof, and R. Mertens, "Micropower energy harvesting," Solid-state Electron., vol. 53, pp.684-693, 2009.

[4] S. P. Beeby, M. J. Tudor, and N. M. White, "Energy harvesting vibration souces for microsystem applications," Meas. Sci. Technol., vol. 17, pp. R175-R195, 2006.

[5] Hagerty J, Helmbrecht F, McCalpin W, Zane R, Popovi&cacute Z. Recycling ambient microwave energy with broad-band rectenna arrays. IEEE Transactions on Microwave Theory and Techniques 2004

[6] P. Glynne-Jones, M. J. Tudor, S. P. Beeby, and N. M. White, "An electromagnetic, vibration-powered generator for intelligent sensor systems," Sens. Actuators, A, vol. 110, pp. 344-349, 2004.

[7] F. Peano and T. Tambosso, "Design and optimization of a MEMS electret-based capacitive energy scavenger," J. Microelectromech. Syst., vol. 14, pp. 435-529, 2005.

[8] D. Shen, S. –Y. Choe, and D. –J. Kim, "Analysis of piezoelectric materials for energy harvesting devices under high-g vibrations," Jpn. J. Appl. Phys., vol. 46, pp. 6755-6760.

[9] S. Roundy and P. K. Wright, "A piezoelectric vibration based generator for wireless electronics," Smart Materials and Structures, vol. 13, pp. 1131-1142, 2004.

[10] Sodano, H.A., Park, G. and Inman D.J. ''A Review of Power Harvesting from Vibration using Piezoelectric Materials,'' The Shock and Vibration Digest, 36(3):197–205, 2004.

[11] Beeby S P, Tudor M J and White N M, "Energy Harvesting vibration sources for Microsystems applications," Meas. Sci.Technol. 17 R175-95, 2006.

[12] S. Roundy, P. K. Wright, and J. Rabaye, "A study of low level vibrations as a power source for wireless sensor nodes," Computer Communications, vol. 26, pp. 1131-1144, 2003.

[13] Don Isarakorn, Thapanun Sudhawiyangkul and Songmoung Nundrakwang, "Energy Analysis in Zigbee based Wireless Sensor Node Powered by Piezoelectric Energy Harveste", Advanced Materials Research Vols. 931-932 (2014) pp 1328-1332.

[14] Suresh Bhalla, Ashok Gupta, Sahil Bansal and Tarun Garg, "Ultra Low-cost Adaptations of Electro-mechanical Impedance Technique for Structural Health Monitoring," Journal of Intelligent Material Systems and Structures May 2009, 20: 991-999.

Final Program

ECTI-CON 2016

ChiangMai Thailand, June 28 - 1 July , 2016

13th International Conference on Electrical Engineering/Electronics Computer, Telecommunications and Information Technology

Illustrated by Assoc.Prof. Wichit Chomtaveewiroot

Rajamangala University of Technology Lanna
ChiangMai, Thailand

Comparative Study of Piezoelectric Energy Harvesters Based on Polycrystalline PZT and Single-crystalline PMN-PT Materials

Phosy Panthongsy
International College
King Mongkut's Institute of Technology Ladkrabang
Bangkok 10520, Thailand

Don Isarakorn
Department of Instrumentation and Control Engineering,
Faculty of Engineering
King Mongkut's Institute of Technology Ladkrabang
Bangkok 10520, Thailand
kidon@kmitl.ac.th

Abstract—**The piezoelectric energy harvester for supplying power to low-power electronic devices, especially low-power wireless sensor node has been studied and received more attraction over the past decade. In order to simplify installation and obtain the sufficient power for systems, the harvester possessing simple structure with highest output power is highly required. The aim of this study is to design and compare the characteristic and performance of piezoelectric polycrystalline PZT and single-crystalline PMN-PT energy harvesters based on unimorph configuration. By utilizing ANSYS® for finite element analysis (FEA), the numerical model of composite piezoelectric unimorph generators with proof mass exciting at resonant frequency 150 Hz are designed and then fabricated. For the energy harvesting experiment, the prototypes of harvesters are mounted to the electromagnetic shaker and inputted the vibration with vary frequencies and accelerations. As the results, the piezoelectric single-crystalline PMN-PT unimorph energy harvester has the higher energy density which is 352.85 J/gm^3, while the piezoelectric polycrystalline PZT unimorph energy harvester has 8.44 J/gm^3.**

Keywords—Finite element analysis; piezoelectric polycrystalline PZT and single-crystalline PMN-PT unimorph energy harvesters; energy harvesting performance.

I. INTRODUCTION

In recent years, wireless sensor technology running on battery is the most commonly utilized for tracing the essential information both in harsh and unreachable environment [1], since the cost is lower than wired solutions due to maintenance, affiliated problem-solving and repair issues. Even though using battery can solve the problem of wiring, it has problem on the limited energy storage capacity. Therefore, the methods converting the waste energy available from the ambient environment into usable electrical energy through the various transduction mechanisms for replacing and prolonging battery on wireless sensor is much challenge and required [2-4]. While there are many approaches to converse the energy; solar [5], thermoelectric [6], electromagnetic [7], electrostatic [8] and piezoelectric conversion [9], piezoelectric energy harvester is giving the best performance [10-14] and popularly studied because of its simple and direct energy conversion from physical deform into electrical energy with high power density [15-16]. Various types of piezoelectric material have been developed to gain more energy from low input frequency and acceleration such piezoelectric polycrystalline PZT and single-crystalline PMN-PT. Both of them having the different piezoelectric and physical properties influence on characteristics and performances of harvesters, particularly piezoelectric strain and electro-mechanical coupling (k_{eff}) coefficient. It leads to achieve the different output electrical energy generation. As a consequence of this, the kind of piezoelectric material providing the sufficient electrical energy is very important for stabilizing the operation of self-powered wireless sensor node.

The purpose of this work is to design, realize and compare the piezoelectric polycrystalline PZT and single-crystalline PMN-PT energy harvesters based on unimorph configuration for harvesting energy from mechanical vibration with low frequency excitation. The harvesters were investigated with an electromagnetic shaker exciting as a mechanical vibration input. The energy harvesting performance of harvesters relating to resonant frequency, mechanical coupling coefficient and electrical energy generation were demonstrated in order to obtain the optimal harvester.

II. DESIGN AND FABRICATION OF PIEZOELECTRIC UNIMORPH ENERGY HARVESTERS

A. Conceptual model

In order to simplify generator configuration, the conceptual model consisting of a piezoelectric unimorph cantilever and beam clamp is designed as shown in Fig. 1. To prevent the clack of piezoelectric, a base of cantilever is attached to acrylic by using mixed resin. Because the high temperature from soldering makes the piezoelectric property change, a PCB clip is directly pinned to piezoelectric surface for avoiding these issues. A piezoelectric unimorph cantilever composes of a piezoelectric layer (1 x 4 x 15 mm^3) bonded to an elastic layer (0.5 x 4 x 40 mm^3); stainless steel plate. An elastic support layer acting as a spring stimulates the neutral plane away from the center of piezoelectric layer thickness. It can cause the net charges be collected. A tungsten proof mass (6 x 6 x 6 mm^3) is placed at the tip of elastic beam for adjusting the natural frequency of harvester.

AUN/SEED-Net, JICA

978-1-4673-9749-0/16/$31.00 ©2016 IEEE

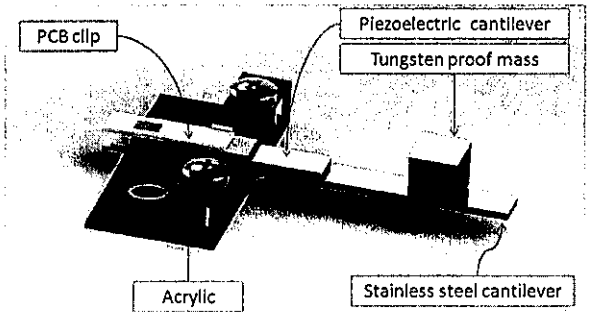

Fig. 1. A conceptual model of piezoelectric unimorph energy harvesters.

B. Finite Element Analysis

As the Fig. 2, the appearance characteristic and resonant excitation of piezoelectric unimorph energy harvesters are designed and estimated in ANSYS. The contributed physical and piezoelectric properties of the materials in simulation are given in Table I. For the harvesters design, resonant frequency of unimorph piezoelectric harvester is one of the most essential parameter. Amount of generated power would be maximized when natural frequency of energy harvesting device matches the frequency of vibration source and it would be decreased when frequency is deviated [14]. Since the frequency ranges of harvestable vibration energy from environment excite between 60 Hz and 200 Hz and its acceleration will decreases with higher frequencies [14], the harvesters are designed to have resonant frequency 150 Hz. A proof mass with a fixed size made of tungsten is directly placed and moved on a stainless steel cantilever in order to tune resonant frequency. By implementing a modal analysis, the composite piezoelectric unimorph harvesters can be obtained as shown in Table II. As the consideration of harvester vibration mode shapes in Fig. 3, the appropriate and homogeneous frequency of harvesters for performance comparison exiting during 60 Hz to 200 Hz is 150.09 Hz.

C. Electromechanical Coupling of Harvesters

From finite element analysis of designed models, the prototypes of piezoelectric unimorph energy harvesters exciting at their resonant frequency 150.09 Hz are fabricated. Their structures were investigated on reverse piezoelectric effect by using impedance analyzer (Type Bode100) to measure the impedance magnitude of harvesters. The impedance analyzer sweeps the frequencies from 100 – 200 Hz with 1 V_{rms} through a reference resistance 50 Ω to harvester.

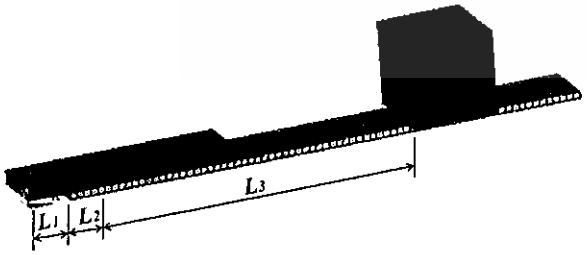

Fig. 2. Configuration of piezoelectric unimorph energy harvester.

TABLE I. PIEZOELECTRIC AND PHYSICAL PROPERTIES FOR NUMERICAL MODEL SIMULATION [17].

Physical and Piezoelectric Properties	Piezoelectric Polycrystalline PZT	Piezoelectric Single-Crystalline PMN-PT	Stainless steel Cantilever (SUS304)	Tungsten
Density(kg m^{-3})	7600	8100	8000	19600
Young's Modulus (GPa)	-	-	190	400
Poisson's Ratio	-	-	0.28	0.28
Piezoelectric Charge Constant [10^{-12} C/N]	$d_{31} = -97$ $d_{33} = 225$ $d_{15} = 330$	$d_{31} = -1338$ $d_{33} = 2820$ $d_{15} = 146$	-	-
Relative Dielectric Constant [ε_0]	$\varepsilon_{11} = 1290$ $\varepsilon_{33} = 1000$	$\varepsilon_{11} = 1600$ $\varepsilon_{33} = 8250$	-	-
Elastic Compliance Constant [10^{-12} m^2/N]	$S_{11}^E = 11.5$ $S_{12}^E = -3.7$ $S_{13}^E = -4.8$ $S_{33}^E = 13.5$ $S_{44}^E = 31.9$ $S_{66}^E = 35.0$	$S_{11}^E = 70.2$ $S_{12}^E = -13.1$ $S_{13}^E = -56.0$ $S_{33}^E = 119.4$ $S_{44}^E = 14.5$ $S_{66}^E = 15.2$	-	-

TABLE II. GLUING RANGE OF THE COMPOSITE PIEZOELECTRIC UNIMORPH CANTILEVER.

Numerical Model of Piezoelectric Unimorph Energy Harvesters	PCB Clipping Length, L1 (mm)	Base Clamping Length, L2 (mm)	Proof mass Placing Length, L3 (mm)
Polycrystalline PZT	3	3	25.41
Single-crystalline PMN-PT	3	3	24.65

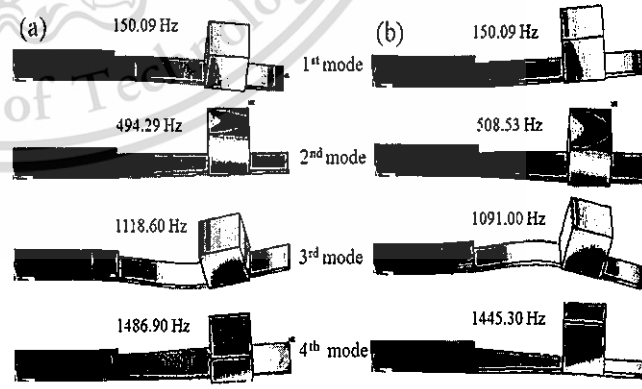

Fig. 3. Vibration mode shapes of the piezoelectric (a) polycrystalline PZT and (b) single-crystalline PMN-PT unimorph energy harvesters.

In Fig. 4 and 5, the measurement results were resonant frequency and anti-resonance frequency. The resonance frequencies of piezoelectric polycrystalline PZT and single-crystalline PMN-PT unimorph energy harvesters resonate at the lowest impedance where 150.33 Hz and 150.48 Hz, and anti-resonant frequencies vibrate at the maximum impedance as 151.51 Hz and 157.20 Hz, respectively. In this case, the electromechanical coupling coefficient presenting the energy conversion ratio can be found by using an equation

$$k_{eff}^2 = 1 - \left(\frac{f_r}{f_a}\right)^2 \quad (1)$$

In this formula, k_{eff} is the mechanical coupling coefficient, f_r is the resonant frequency, and f_a is anti-resonant frequency of harvester.

III. Energy Harvesting Experimental Setup

To investigate the energy harvesting performance of piezoelectric unimorph energy harvesters, their prototypes are mounted to an electromagnetic shaker (Bruel & Kjaer type 4810). Vary acceleration levels from 0.1 – 0.7 g and excitation frequencies during 120 – 180 Hz applying as the mechanical vibration input to harvesters are driven by a power amplifier (Type 2706) and a function generator (Agilent type 33120A). An accelerometer is attached to vibration source for monitoring the magnitude of accelerations, and frequencies as show in Fig. 6.

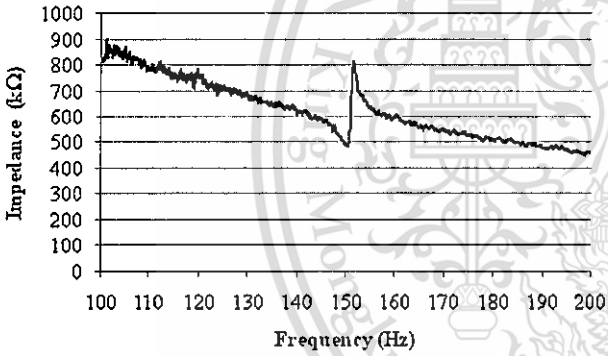

Fig. 4. Impedance measurement result of piezoelectric polycrystalline PZT unimorph energy harvester.

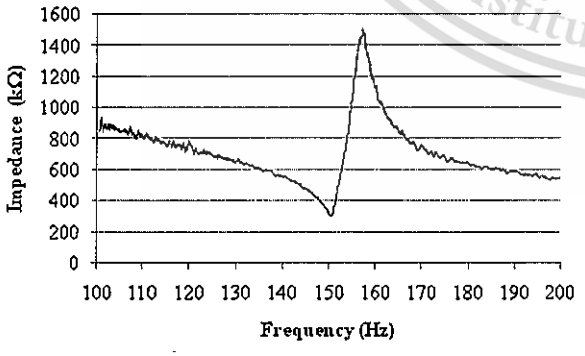

Fig. 5. Impedance measurement result of piezoelectric single-crystalline PMN-PT unimorph energy harvester.

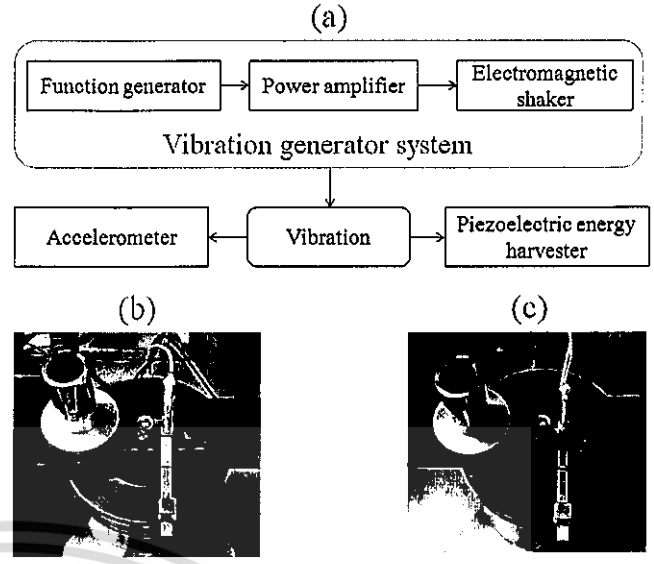

Fig. 6. (a) A flow chart of energy harvesting experimental setup, and the prototype of piezoelectric (b) polycrystalline PZT and (c) single-crystalline PMN-PT unimorph energy harvesters.

IV. Results and Discussion

As the energy harvesting experiment results of the prototypes of piezoelectric polycrystalline PZT and single-crystalline PMN-PT unimorph energy harvesters are illustrated in the Fig. 7 and 8. The frequencies of harvesters are decreased by increasing the acceleration magnitude of vibration source. It demonstrates that the young's modulus of harvesters was reduced. The cause of this decrease was depended on the limitation of piezoelectric compliance under heavy stress [18]. While an electromagnetic shaker vibrate at 0.1 g acceleration, piezoelectric polycrystalline PZT and single-crystalline PMN-PT unimorph energy harvesters generate the maximum AC voltage 4.09 V and 18.11 V at 150 Hz. By shaking 0.7 g acceleration, the generated maximum AC voltages are 20.12 V and 105.60 V at 144.10 Hz and 147.50 Hz, respectively.

One of the most important parameters for considering the energy transduction capacity of the resonant type piezoelectric energy harvesters is quality factor (Q). The Q factor is estimated by

$$Q = \frac{f_r}{f_2 - f_1} \quad (2)$$

where, f_r is the resonant frequency of harvester, and $f_2 - f_1$ is the range of frequency values (bandwidth) where the 0.707 times of the generated voltage amplitude at resonant frequency.

From a formula (2), a high Q factor obtaining from a narrow bandwidth demonstrates that the harvester is very reactive to the vibration change. In the meantime, the energy also can be harvested in a cramped frequency range around the resonant frequency.

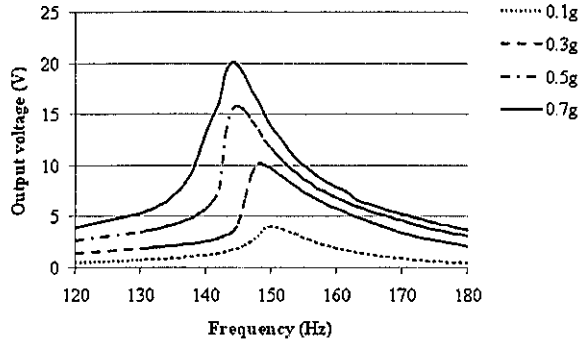

Fig. 7. Generated output voltage of piezoelectric polycrystalline PZT unimorph energy harvester.

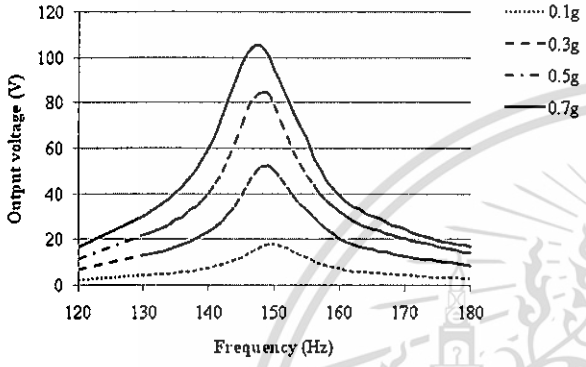

Fig. 8. Generated output voltage of piezoelectric single-crystalline PMN-PT unimorph energy harvester.

A low Q factor presents the harvestable energy in the large frequency range about the resonant frequency range due to a large bandwidth frequency. The piezoelectric polycrystalline PZT and single-crystalline PMN-PT unimorph energy harvesters have the quality factor as 19.73 and 16.85 while being excited at 0.1 g, serially.

Since the characteristics of piezoelectric energy harvesters are fundamentally capacitor, their capacitances were found for examining the generated energy by using an equation

$$C_p = \varepsilon_r \varepsilon_0 \frac{A}{t} \tag{3}$$

where, C_p is the capacitance of harvesters, ε_r is the relative dielectric constant, ε_0 is the permittivity of free space (ε_0 = 8.85 x 10^{-12} F/m), A is a piezoelectric surface area (electrode surface area), and t is a thickness of piezoelectric (thickness separating the electrodes).

Thus, the generated energy is given by

$$E = \frac{1}{2} C_p V^2 \tag{4}$$

In this equation, E is the generated energy, C_p is the capacitance of harvesters, and V is the generated voltage.

Following the harvestable energy graph in Fig. 9, a piezoelectric single-crystalline PMN-PT unimorph energy harvester has the higher energy density as 7.26 J/m^3 at 0.1 g

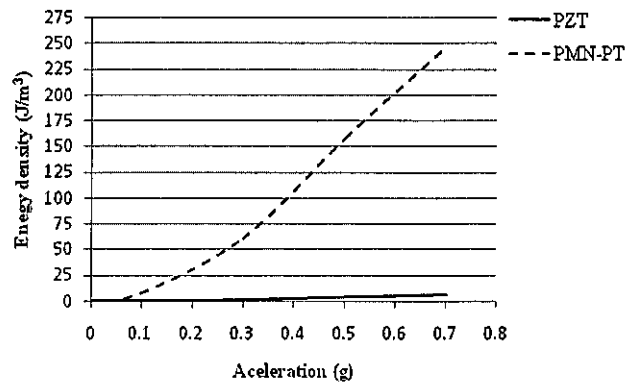

Fig. 9. Energy density of harvesters with different acceleration levels.

TABLE III. PERFORMANCE COMPARISON.

Performance parameters	Polycrystalline PZT	Single-crystalline PMN-PT
Coupling Coefficient (k_{eff})	0.14	0.30
Quality Factor (Q)	197.30 g^{-1}	168.50 g^{-1}
Capacitance (C_p)	1.75 nF	2.66 nF
Voltage (V)	40.90 V g^{-1}	181.10 V g^{-1}
Energy Density (E)	8.44 J/g m^3	352.85 J/g m^3

and it significantly increase to 247 J/m^3 at 0.7 g, while the energy density of piezoelectric polycrystalline PZT unimorph energy harvester is 0.24 J/m^3 at 0.1 g and 5.91 J/m^3 at 0.7 g.

Most of the important parameters for comparison of piezoelectric polycrystalline PZT and single-crystalline PMN-PT unimorph energy harvesters were demonstrated in Table III. A piezoelectric single-crystalline PMN-PT material is more appropriate to be fabricated the unimorph energy harvester then polycrystalline PZT material due to its greater performance.

V. CONCLUSION

The study on the piezoelectric polycrystalline PZT and single-crystalline PMN-PT unimorph energy harvesters focusing on design and performance comparison were presented in this paper. The designed models were investigated by using finite element method (FEM). The simulation results show the appropriate vibration shape of the models exciting at 50.09 Hz for harvester fabrication. A comparative study of harvester prototypes were done by following the parameters of electromechanical coupling coefficient, quality factor, capacitance, generated voltage and energy density. A performance comparison expresses that, a piezoelectric single-crystalline PMN-PT unimorph energy harvester is an optimal

one with the highest energy density (352.85 J/gm^3), while piezoelectric polycrystalline PZT unimorph energy harvester has the energy density (8.44 J/gm^3).

ACKNOWLEDGMENT

Mr. Phosy Panthongsy would like to express sincere appreciation to the AUN/SEED-Net for the fully financial support in his master degree education and acknowledge to King Mongkut's Institute of Technology Ladkrabang (KMITL), Bangkok, Thailand for supplying the excellent research facilities.

REFERENCES

[1] V. C. Gungor and G. P. Hancke, "Industrial wireless sensor networks:Challenges, design principles, and technical approaches," IEEE Trans. Ind. Electron., Vol. 56, No. 10, pp. 4258–4265, October 2009.

[2] Yen Kheng Tan and Sanjib Kumar Panda, "Energy Harvesting From Hybrid Indoor Ambient Light and Thermal Energy Sources for Enhanced Performance of Wireless Sensor Nodes," IEEE TRANSACTIONS ON INDUSTRIAL ELECTRONICS, Vol. 58, No. 9, pp. 4424 – 4435, September 2011.

[3] Paul D. Mitcheson and el at, "Energy Harvesting From Human and MachineMotion for Wireless Electronic Devices," Proceeding of the IEEE, Vol.96, No.9, pp. 1457-1486, 2008.

[4] Jianmin Hou and Yi Gao, "Greenhouse Wireless Sensor Network Monitoring System Design Based on Solar Energy," 2010 International Conference on Challenges in Environmental Science and Computer Engineering, pp. 475-479, 2010.

[5] D. Brunelli, L. Benini, C. Moser, L. Thiele, "An Efficient Solar Energy Harvester for Wireless Sensor Nodes," Design, Automation and Test in Europe, March 2008.

[6] R. J. M. Vullers, R. Van Schaijk, I. Doms, C. Van Hoof, and R. Mertens, "Micro power energy harvesting," Solid-state Electron., Vol. 53, pp.684-693, 2009.

[7] P. Glynne-Jones, M. J. Tudor, S. P. Beeby, and N. M. White, "An electromagnetic, vibration-powered generator for intelligent sensor systems," Sens. Actuators, A, Vol. 110, pp. 344-349, 2004.

[8] F. Peano and T. Tambosso, "Design and optimization of a MEMS electret-based capacitive energy scavenger," J. Microelectromech. Syst., Vol. 14, pp. 435-529, 2005.

[9] D. Shen, S. –Y. Choe, and D. –J. Kim, "Analysis of piezoelectric materials for energy harvesting devices under high-g vibrations," Jpn. J. Appl. Phys., Vol. 46, pp. 6755-6760.

[10] Schmidt V H 1986 "Theoretical electrical power output per unit volume of PVF2 and mechanical-to-electrical conversion efficiency as functions of frequency," Proc. 6th IEEE Int. Symp. on Applications of Ferroelectrics, pp. 538–42.

[11] Shenck N S and Paradiso J A 2001, "Energy scavenging with shoe-mounted piezoelectrics," IEEE Micr, Vol. 21, pp.30–41.

[12] Glynne-Jones P, Beeby S P, James E P and White N M 2001, "The modelling of a piezoelectric vibration powered generator for Microsystems," Transducers 01/Eurosensors XV , June 2001.

[13] Ottman G K, Hofmann H F and Lesieutre G A 2003, "Optimized piezoelectric energy harvesting circuit using step-down converter in discontinuous conduction mode," IEEE Trans. Power Electron. Vol.18, pp. 696–703.

[14] S. Roundy, P. K. Wright, and J. Rabaye, "A study of low level vibrations as a power source for wireless sensor nodes," Computer Communications, Vol. 26, pp. 1131-1144, 2003.

[15] Sodano, H.A., Park, G. and Inman D.J. ''A Review of Power Harvesting from Vibration using Piezoelectric Materials,'' The Shock and Vibration Digest, Vol. 36(3), pp. 197–205, 2004.

[16] S. Roundy and P. K. Wright, "A piezoelectric vibration based generator for wireless electronics," Smart Materials and Structures, Vol. 13, pp. 1131-1142, 2004.

[17] K.C. Kim, Y.S. Kim, H.J. Kim, S.H. Kim "Finite element analysis of piezoelectric actuator with PMN–PT single crystals for nanopositioning," Current Applied Physics, Vol. 6, pp. 1064–1067, October 2006.

[18] D. Shen, J.-H. Park, J. Ajitsaria, S.-Y. Choe, H.C. Wikle III, D.-J. Kim, "The design, fabrication and evaluation of a MEMS PZT cantilever with an integrated Si proof mass for vibration energy harvesting," J. Micromech. Microeng., Vol. 18, No. 5, Article No. 055017, 2008.

APPENDIX B

Author Biography

Name: Mr. Phosy Panthongsy

Date of Birth: September 9th, 1992

Born: Houaphan Province, LAOS

Current Address: 509/23 Saphanthongtai Village, Sisattanark District, Vientiane Capital, LAOS

E-mail: phosy_pts@hotmail.com

Qualification

Education

- Bachelor Degree of Electronic Engineering, National University of Laos, LAOS, in 2014

Skilled Works

- Computer Programming
- Energy Harvesting
- Piezoelectric Harvester
- Robotic